

Decentralized Stochastic Optimization over Unreliable Networks via Two-timescales Updates

Haoming Liu, Chung-Yiu Yau, Hoi-To Wai, *Member, IEEE*

Abstract—This paper introduces a robust two-timescale compressed primal-dual (TiCoPD) algorithm tailored for decentralized optimization under bandwidth-limited and unreliable channels. By integrating the majorization-minimization approach with the primal-dual optimization framework, the TiCoPD algorithm strategically compresses the difference term shared among agents to enhance communication efficiency and robustness against noisy channels without compromising convergence stability. The method incorporates a mirror sequence for agent consensus on nonlinearly compressed terms updated on a fast timescale, together with a slow timescale primal-dual recursion for optimizing the objective function. Our analysis demonstrates that the proposed algorithm converges to a stationary solution when the objective function is smooth but possibly non-convex. Numerical experiments corroborate the conclusions of this paper.

Index Terms—Distributed Optimization, Consensus Optimization, Two-timescale Iteration.

I. INTRODUCTION

Many problems in signal processing and machine learning can be handled by tackling the optimization problem:

$$\min_{\mathbf{x} \in \mathbb{R}^d} f(\mathbf{x}) := \frac{1}{n} \sum_{i=1}^n f_i(\mathbf{x}), \quad (1)$$

where for each $i \in [n] := \{1, \dots, n\}$, $f_i : \mathbb{R}^d \rightarrow \mathbb{R}$ is a continuously differentiable function, and n is the number of agents. For example, f_i is the cross-entropy loss for learning a neural network classifier model, defined on the i th partition of data. We consider a distributed optimization setting where f_i is a local objective function held by the i th agent that is not shared with other agents. The local data available at the agents are typically heterogeneous, i.e., f_i are distinct from others. Instead of relying on a central server that is connected to all agents, (1) shall be handled by the cooperation between the n agents. Distributed algorithms for (1) have been developed actively, such as in signal processing for tackling the estimation problem in wireless sensor networks in privacy and bandwidth sensitive applications [1]–[3], and in machine learning for parallel computation [4], [5].

Decentralized optimization algorithms that can operate with on-device computation and local communication with a subset of agents are preferred for problem (1). To this end, a popular approach is to mimick the (centralized) gradient method where agents perform gradient update with the local objective functions while performing a consensus step with neighbors. This leads to primal-only schemes such as decentralized gradient

(DGD) method [6]–[9] as well as the popular extensions such as gradient tracking, EXTRA [7], [8]. Another approach is the (proximal) primal-dual algorithm [10], [11] which features a primal-dual descent-ascent method developed by viewing (1) as a consensus-constrained optimization problem. The primal-dual framework also generalizes primal-only schemes such as EXTRA, gradient tracking, and have been demonstrated to exhibit fast convergence under mild conditions [12].

For application scenarios such as wireless sensor networks, the communication channels between agents can be prone to (i) *link failures*, (ii) *bandwidth limitation*, and (iii) *noise perturbation*. To this end, an important objective is to robustify the decentralized optimization algorithms for *unreliable networks*. The case of time-varying networks which models link failures has been studied in [13], [14] for DGD and gradient tracking methods. For bandwidth-limited networks, earlier works [15]–[17] have proposed to combine distributed optimization algorithms with quantized communication that achieves acceptable performance in numerical experiments, [18], [19] have studied error feedback subroutines with theoretically guaranteed exact convergence. More recently, [20]–[23] considered modifications of DGD and gradient tracking algorithms with error feedback subroutines, [24]–[27] have studied their stochastic gradient extensions, and [28] developed a primal-dual algorithm that supports random with sparsified communication. For noisy communication networks, [29], [30] considered a two-timescales update mechanism to modify the DGD algorithm for controlling the noise variance. With a similar motivation, [31]–[33] have studied information theoretical limits under finite-bit transmission induced by noisy channels.

In addition to focusing on only one or two specific issues in unreliable networks, the theoretical guarantees available for the above decentralized algorithms are quite restrictive. For instance, the convergence of CHOCO-SGD algorithm [24] requires a bounded heterogeneity assumption and converges slowly when agent’s data distribution are highly heterogeneous; the CP-SGD algorithm [27] exhibits faster convergence, but does not support time-varying graphs and noisy compressed transmission; the FSPDA algorithm [28] only supports random sparsification as compression scheme with noiseless communication.

The above motivates the current work to design fast-converging decentralized optimization algorithms that are robust to unreliable networks. We notice several challenges. To combat data heterogeneity, one cannot rely on simple schemes such as the plain DGD algorithm. Instead, a possible solution is to utilize the primal-dual (PD) optimization framework that can naturally lead to a decentralized algorithm which con-

HL, CYY, HTW are with the Dept. of SEEM, CUHK. This research is supported in part by project #MMT-p5-23 of the Shun Hing Institute of Advanced Engineering, The Chinese University of Hong Kong.

Prior Works	Bounded Heterogeneity	Random Graph	Compression	Noisy Communication	Convergence Rate (Noiseless Comm.)	Convergence Rate (Noisy Comm.)
CHOCO-SGD [24]	required	restricted	contractive	✗	$\mathcal{O}(\bar{\sigma}/\sqrt{nT})$	/
DIMIX [30]	required	unrestricted	contractive	✓	/	$\mathcal{O}(T^{-1/3} \ln T)$
CP-SGD [27]	not required	restricted	contractive	✗	$\mathcal{O}(1/\sqrt{nT})$	/
FSPDA [28]	not required	unrestricted	sparsification	✗	$\mathcal{O}(\bar{\sigma}/\sqrt{nT})$	/
This Work	not required	unrestricted	contractive	✓	$\mathcal{O}(\bar{\sigma}/\sqrt{nT})$	$\mathcal{O}(n^{-1/2}T^{-1/3})$

TABLE I
COMPARISON OF TiCoPD TO STATE-OF-THE-ART DECENTRALIZED ALGORITHMS FOR NON-CONVEX STOCHASTIC OPTIMIZATION.

verges regardless of the degree of data heterogeneity. However, the PD algorithm design lacks a natural recipe to deal with link failure and noisy communication as the algorithm is not integrated with a consensus subroutine.

To this end, we design a new decentralized algorithm with two ingredients: (A) a majorization-minimization procedure and (B) a two-timescale updating scheme for average consensus. The first component allows for randomness due to link failure in the communication network and separates the decision variables and the variables to be transmitted. The second component is inspired by the *nonlinear gossiping* framework [34] which replaces the classical linear average consensus map with a suitably designed nonlinear map for average consensus. The general idea is to observe that the nonlinear map converges at a faster rate than the stochastic approximation step in a consensus algorithm. In our case, we design the said nonlinear map with a compression operator applied to a *compression error vector* to combat with limited bandwidth, while simultaneously allow for additive noise in the operation that handles noisy channels.

This paper aims at developing a stochastic primal-dual algorithm for (1) that is robust to unreliable networks. Our contributions are summarized as:

- We propose the **Two-timescale Compressed stochastic Primal-Dual (TiCoPD)** algorithm. The TiCoPD algorithm follows a two-level update which separates *communication* and *optimization* steps, and handle them using two timescale updates. To our best knowledge, this is the first nonlinearly compressed stochastic primal-dual algorithm for decentralized optimization on random graphs.
- To incorporate nonlinear compression into the decentralized algorithm, we develop a (stochastic) majorization-minimization (MM) procedure which suggests agents to transmit the compressed difference terms. This offers a new perspective for understanding the error feedback mechanism developed in [24] and draws connection to the nonlinear gossiping algorithm [34]. We believe that this observation is of independent interest.
- For optimization problems with continuously differentiable (possibly non-convex) objective functions, we show that with noiseless compressed transmission, the TiCoPD algorithm converges in expectation – in T iterations, it finds a solution $\bar{\mathbf{X}}$ that is $\mathcal{O}(1/\sqrt{nT})$ -stationary. The rate is comparable to that of a centralized SGD algorithm asymptotically. With noisy compressed transmission, we show that the TiCoPD algorithm finds an $\mathcal{O}(1/T^{1/3})$ -stationary solution in T iterations. The rate is faster

than DIMIX [30], and does not require the bounded heterogeneity assumption.

Table I compares TiCoPD to existing algorithms. Observe that the latter has the fastest convergence rate with the least restrictions on compressor design and data requirement. Compared to the conference version [35], we have extended the TiCoPD algorithm to work with stochastic gradients and unreliable network environments, together with a new set of experiments.

The rest of this paper is organized as follows. Section II introduces the primal-dual framework of distributed optimization. Section III provides the derivation of two-timescales update and majorization-minimization, and develops the TiCoPD algorithm. Section IV presents the convergence analysis of TiCoPD. Section V provides the numerical experiments. Finally, Section VI concludes the paper.

Notations. Let $\mathbf{K} \in \mathbb{R}^{d \times d}$ be a symmetric matrix, the \mathbf{K} -weighted inner product of vectors $\mathbf{a}, \mathbf{b} \in \mathbb{R}^d$ is denoted as $\langle \mathbf{a} | \mathbf{b} \rangle_{\mathbf{K}} := \mathbf{a}^\top \mathbf{K} \mathbf{b}$. Similarly, the \mathbf{K} -weighted norm is denoted by $\|\mathbf{a}\|_{\mathbf{K}}^2 := \mathbf{a}^\top \mathbf{K} \mathbf{a}$. $(\cdot)^\dagger$ denotes the Moore-Penrose inverse of the matrix. $\lfloor \cdot \rfloor$ denotes the floor function.

II. PROBLEM STATEMENT

Let $G = (V, E)$ be an undirected and connected graph of the agent set $V = \{1, \dots, n\}$, and $E \subseteq V \times V$ is the set of usable edges between the n agents. The graph G is also endowed with an incidence matrix $\mathbf{A} \in \mathbb{R}^{|E| \times n}$ and we shall denote $\bar{\mathbf{A}} := \mathbf{A} \otimes \mathbf{I}_d$, where \otimes denotes the Kronecker product.

We consider a setting where both the optimization problem (1) and the graph are stochastic. Let the probability space be $(\Omega, \mathcal{F}, \mathbb{P})$, where $\Omega := \Omega_1 \times \dots \times \Omega_n \times \Omega_A$ is the sample space. For each $i \in V$, $\xi_i \in \Omega_i$ admits the distribution \mathbb{P}_i that leads to the i th local objective function:

$$f_i(\mathbf{x}_i) := \mathbb{E}_{\xi_i \sim \mathbb{P}_i} [f_i(\mathbf{x}_i; \xi_i)]. \quad (2)$$

With a slight abuse of notation, we also used f_i as the measurable function $f_i : \mathbb{R}^d \times \Omega_i \rightarrow \mathbb{R}$ such that its second argument represents a random sample. To define the stochastic graph model, we consider $\xi_a \sim \mathbb{P}_A$ and define a subgraph selection diagonal matrix $\mathbf{I}(\xi_a) \in \{0, 1\}^{|E| \times |E|}$. The corresponding subgraph is then denoted as $\mathcal{G}(\xi_a) = (V, E(\xi_a))$ with $E(\xi_a) \subseteq E$. We have $\mathbb{E}_{\xi_a \sim \mathbb{P}_A} [\mathbf{I}(\xi_a)] > c \mathbf{I}_{|E|}$ for some $c > 0$ such that each edge is selected with a non-zero probability. To simplify notation, we let $\mathbf{X} = [\mathbf{x}_1; \dots; \mathbf{x}_n] \in \mathbb{R}^{nd}$.

We observe that (1) is equivalent to the stochastic equality constrained optimization problem:

$$\min_{\mathbf{X} \in \mathbb{R}^{nd}} \frac{1}{n} \sum_{i=1}^n f_i(\mathbf{x}_i) \quad \text{s.t.} \quad \mathbb{E}_{\xi_a \sim \mathbb{P}_A} [\bar{\mathbf{A}}(\xi_a)] \mathbf{X} = 0, \quad (3)$$

where we have defined $\bar{\mathbf{A}}(\xi_a) = (\mathbf{I}(\xi_a)\mathbf{A}) \otimes \mathbf{I}_d$ to be the incidence matrix for a *random subgraph* of G . We denote $\nabla \mathbf{f}(\mathbf{X}; \xi) \in \mathbb{R}^{nd}$ as the stack of the local stochastic gradients $\nabla f_i(\mathbf{x}_i; \xi_i)$, and $\nabla \mathbf{f}(\mathbf{X}) \in \mathbb{R}^{nd}$ as the stack of the local expected gradients $\nabla f_i(\mathbf{x}_i)$. To simplify notations, we denote

$$f(\bar{\mathbf{x}}) := \frac{1}{n} \sum_{i=1}^n f_i(\bar{\mathbf{x}}), \quad \nabla f(\bar{\mathbf{x}}) := \frac{1}{n} \sum_{i=1}^n \nabla f_i(\bar{\mathbf{x}}), \quad (4)$$

as the global objective function and exact global gradient evaluated on a common decision variable $\bar{\mathbf{x}} \in \mathbb{R}^d$.

A. Proximal Gradient Primal-dual Algorithm

Before introducing the main idea of TiCoPD, we consider adopting the Prox-GPDA algorithm [10] to the stochastic problem (3) to illustrate how the primal-dual approach can naturally lead to a decentralized optimization algorithm. Meanwhile, we highlight the difficulties in adapting the existing algorithm for unreliable networks.

As the first step, consider the following sampled augmented Lagrangian function of (3):

$$\mathcal{L}(\mathbf{X}, \boldsymbol{\lambda}; \xi) := \frac{1}{n} \sum_{i=1}^n f_i(\mathbf{x}_i; \xi_i) + \boldsymbol{\lambda}^\top \bar{\mathbf{A}}(\xi_a) \mathbf{X} + \frac{\theta}{2} \|\bar{\mathbf{A}}(\xi_a) \mathbf{X}\|^2, \quad (5)$$

where $\boldsymbol{\lambda} = (\boldsymbol{\lambda}_i)_{i \in E} \in \mathbb{R}^{|E|d}$ is the Lagrange multiplier for the equality constraint and $\theta > 0$ is a regularization parameter.

Denote $\xi^{t+1} \sim \mathbb{P}$ as the random variables drawn at iteration t and let $(\mathbf{X}^t, \boldsymbol{\lambda}^t)$ be the t th primal-dual iterates. By partially linearizing $f_i(\cdot; \xi_i^{t+1})$ and including the weighted proximal term suggested in [10], the primal-dual update at iteration $t \geq 0$ can be expressed as,

$$\begin{aligned} \mathbf{X}^{t+1} = \arg \min_{\mathbf{X} \in \mathbb{R}^{nd}} & \nabla \mathbf{f}(\mathbf{X}^t; \xi^{t+1})^\top (\mathbf{X} - \mathbf{X}^t) + \mathbf{X}^\top \bar{\mathbf{A}}(\xi_a^{t+1}) \boldsymbol{\lambda}^t \\ & + \frac{\theta}{2} \|\bar{\mathbf{A}}(\xi_a^{t+1}) \mathbf{X}\|^2 + \frac{1}{2} \|\mathbf{X} - \mathbf{X}^t\|_{\tilde{\alpha}^{-1} \mathbf{I} + \mathbf{B}(\xi_a^{t+1})}^2, \end{aligned} \quad (6)$$

$$\boldsymbol{\lambda}^{t+1} = \arg \min_{\boldsymbol{\lambda} \in \mathbb{R}^{nd}} -\boldsymbol{\lambda}^\top \bar{\mathbf{A}}(\xi_a^{t+1}) \mathbf{X}^t + \frac{1}{2\eta} \|\boldsymbol{\lambda} - \boldsymbol{\lambda}^t\|^2. \quad (7)$$

with Laplacian of the subgraph $\tilde{\mathbf{L}}(\xi_a) := \bar{\mathbf{A}}^\top \bar{\mathbf{A}}(\xi_a)$ and

$$\mathbf{B}(\xi_a) = \theta(2 \text{Diag}(\tilde{\mathbf{L}}(\xi_a)) - \tilde{\mathbf{L}}(\xi_a)), \quad (8)$$

This leads to the following Prox-GPDA recursion:

$$\begin{aligned} \mathbf{X}^{t+1} = \mathbf{D}(\xi_a^{t+1})^{-1} & ((\mathbf{I}_{nd} + \tilde{\alpha} \mathbf{B}(\xi_a^{t+1})) \mathbf{X}^t \\ & - \tilde{\alpha} \nabla \mathbf{f}(\mathbf{X}^t; \xi^{t+1}) - \tilde{\alpha} \bar{\mathbf{A}}(\xi_a^{t+1})^\top \boldsymbol{\lambda}^t) \end{aligned} \quad (9)$$

$$\boldsymbol{\lambda}^{t+1} = \boldsymbol{\lambda}^t + \eta \bar{\mathbf{A}}(\xi_a^{t+1}) \mathbf{X}^t, \quad (10)$$

where $\mathbf{D}(\xi_a^{t+1}) = 2\tilde{\alpha}\theta \text{Diag}(\tilde{\mathbf{L}}(\xi_a^{t+1})) + \mathbf{I}_{nd}$ is diagonal.

We notice that (9), (10) incorporate both *communication* and *optimization* steps in a single update: in particular, let $d_{ii}^{t+1}, L_{ii}^{t+1}$ be the i th diagonal element of $\mathbf{D}(\xi_a^{t+1}), \tilde{\mathbf{L}}(\xi_a^{t+1})$,

$$\begin{aligned} \mathbf{x}_i^{t+1} = & \underbrace{(d_{ii}^{t+1})^{-1} [(1 + 2\tilde{\alpha}\theta L_{ii}^{t+1}) \mathbf{x}_i^t - \tilde{\alpha} \nabla f_i(\mathbf{x}_i^t; \xi_i^{t+1})]}_{\text{(local) optimization step}} \\ & - (d_{ii}^{t+1})^{-1} \underbrace{\left[\tilde{\alpha}\theta \sum_{j \in \mathcal{N}_i^t} (\mathbf{x}_j^t - \mathbf{x}_i^t) + \tilde{\alpha} \sum_{(i,j): j \in \mathcal{N}_i^t} \boldsymbol{\lambda}_{(i,j)}^t \right]}_{\text{communication step}} \end{aligned}$$

and similar observations can be made for the $\boldsymbol{\lambda}$ -update. As observed by [36], this modification of Prox-GPDA can be implemented on random graphs, although its analysis involves a significantly different approach from [10].

However, Prox-GPDA (9), (10) may not be suitable for unreliable networks, where it requires transmitting a message of d real numbers on each activated edge at every iteration. In instances of (3) with $d \gg 1$, this results in a significant bandwidth usage. As discussed in the Introduction, a remedy is to compress each transmitted message such as quantizing the real numbers into a small number of bits before transmission. That being said, directly incorporating a compression operator into the recursion may result in non-convergence.

III. TWO-TIMESCALE COMPRESSED STOCHASTIC PRIMAL-DUAL ALGORITHM

This section develops the **Two-timescale Compressed stochastic Primal-Dual (TiCoPD)** algorithm as a perturbed version of (9), (10). Our key idea is to treat *compressed communication* and *optimization* as updates at the lower and upper levels, respectively. The algorithm depends on two ingredients: (i) a majorization-minimization step that introduces a *surrogate* variable to separate the communication step from the optimization step, (ii) a *two-timescales* update that incorporates a *noisy* and *nonlinearly compressed* update of the surrogate variable through compressed message exchanges.

We develop the algorithm by revisiting the update structure in (6), (7). The gradient of $\|\bar{\mathbf{A}}(\xi) \mathbf{X}\|^2$ w.r.t. \mathbf{x}_i takes the form

$$\sum_{j \in \mathcal{N}_i(\xi)} (\mathbf{x}_i - \mathbf{x}_j) \quad (11)$$

whose evaluation necessitates the communication of the neighbors' decision variables \mathbf{x}_j , $j \in \mathcal{N}_i(\xi)$. This results in a communication bottleneck that demands the transmission of d dimensional decision variables, as discussed in the previous section. Our idea is to sidestep this term through an MM procedure defined with a surrogate variable. To this end, we consider the mirror sequence $\{\hat{\mathbf{X}}^t\}_{t \geq 0}$ such that (i) $\hat{\mathbf{X}}^t \approx \mathbf{X}^t$, and (ii) it is possible for agent i to acquire the neighbors' surrogate variables $(\hat{\mathbf{x}}_j^t)_{j \in \mathcal{N}_i^t}$ with *compressed communication*. We will illustrate how to construct such mirror sequence later.

Majorization-Minimization. To derive the \mathbf{X} -subproblem for TiCoPD, we first consider linearizing the $\|\bar{\mathbf{A}}(\xi_a) \mathbf{X}\|^2$ term in (6) w.r.t. a fixed \mathbf{X}^t and observe that there exists $M \geq 0$ where

$$\|\bar{\mathbf{A}}(\xi_a) \mathbf{X}\|^2 \leq (\bar{\mathbf{A}}^\top \bar{\mathbf{A}}(\xi_a) \mathbf{X}^t)^\top (\mathbf{X} - \mathbf{X}^t) + \frac{M}{2} \|\mathbf{X} - \mathbf{X}^t\|^2,$$

for any $\mathbf{X} \in \mathbb{R}^{nd}$. Furthermore, it holds

$$\begin{aligned} (\bar{\mathbf{A}}^\top \bar{\mathbf{A}}(\xi_a) \mathbf{X}^t)^\top (\mathbf{X} - \mathbf{X}^t) &= (\bar{\mathbf{A}}^\top \bar{\mathbf{A}}(\xi_a) \hat{\mathbf{X}}^t)^\top (\mathbf{X} - \mathbf{X}^t) \\ &\quad + (\bar{\mathbf{A}}^\top \bar{\mathbf{A}}(\xi_a) (\mathbf{X}^t - \hat{\mathbf{X}}^t))^\top (\mathbf{X} - \mathbf{X}^t) \\ &\leq (\bar{\mathbf{A}}^\top \bar{\mathbf{A}}(\xi_a) \hat{\mathbf{X}}^t)^\top (\mathbf{X} - \mathbf{X}^t) \\ &\quad + \frac{1}{2} \|\bar{\mathbf{A}}^\top \bar{\mathbf{A}}(\xi_a) (\mathbf{X}^t - \hat{\mathbf{X}}^t)\|_F^2 + \frac{1}{2} \|\mathbf{X} - \mathbf{X}^t\|^2. \end{aligned}$$

The TiCoPD algorithm thus obtains \mathbf{X}^{t+1} via minimizing a majorized version of the objective function in (6)¹:

$$\begin{aligned} \mathbf{X}^{t+1} = \arg \min_{\mathbf{X} \in \mathbb{R}^{nd}} & \mathbf{X}^\top (\nabla \mathbf{f}(\mathbf{X}^t; \xi^{t+1}) + \bar{\mathbf{A}}(\xi_a^{t+1}) \boldsymbol{\lambda}^t) \\ & + \theta \mathbf{X}^\top \tilde{\mathbf{L}}(\xi_a^{t+1}) \hat{\mathbf{X}}^t + \frac{\theta \tilde{\alpha}(M+1) + 1}{2\tilde{\alpha}} \|\mathbf{X} - \mathbf{X}^t\|^2. \end{aligned} \quad (12)$$

For the $\boldsymbol{\lambda}$ -subproblem, we similarly replace \mathbf{X}^t with the surrogate variable $\hat{\mathbf{X}}^t$. We obtain:

$$\boldsymbol{\lambda}^{t+1} = \arg \min_{\boldsymbol{\lambda} \in \mathbb{R}^{d|E|}} \frac{1}{2\eta} \|\boldsymbol{\lambda} - \boldsymbol{\lambda}^t\|^2 - \boldsymbol{\lambda}^\top \bar{\mathbf{A}}(\xi_a^{t+1}) \hat{\mathbf{X}}^t, \quad (13)$$

Finally, by the variable substitution $\tilde{\boldsymbol{\lambda}}^t = \bar{\mathbf{A}}^\top \boldsymbol{\lambda}^t$, the TiCoPD algorithm uses the following recursion for updating the primal-dual variables:

$$\begin{aligned} \mathbf{X}^{t+1} &= \mathbf{X}^t - \alpha [\nabla \mathbf{f}(\mathbf{X}^t; \xi^{t+1}) + \tilde{\boldsymbol{\lambda}}^t + \theta \tilde{\mathbf{L}}(\xi_a^{t+1}) \hat{\mathbf{X}}^t], \\ \tilde{\boldsymbol{\lambda}}^{t+1} &= \tilde{\boldsymbol{\lambda}}^t + \eta \tilde{\mathbf{L}}(\xi_a^{t+1}) \hat{\mathbf{X}}^t, \end{aligned} \quad (14)$$

with $\alpha = \frac{1}{\frac{1}{\tilde{\alpha}} + \theta(M+1)}$. Recall that $\bar{\mathbf{A}}$ is the incidence matrix where the i th block of $\tilde{\mathbf{L}}(\xi_a^{t+1}) \hat{\mathbf{X}}^t$ reads $\sum_{j \in \mathcal{N}_i^t} (\hat{\mathbf{x}}_j^t - \hat{\mathbf{x}}_i^t)$, where $\mathcal{N}_i^t := \mathcal{N}_i(\xi_a^{t+1})$ is the neighborhood of agent i at iteration t . It can be seen that the updates of \mathbf{X}^t and $\tilde{\boldsymbol{\lambda}}^t$ require only transmitting the surrogate variables $\hat{\mathbf{x}}_1^t, \dots, \hat{\mathbf{x}}_n^t$. Next, we will design a procedure to enable the latter with only compressed communication.

Two-timescales Update. Our next endeavor is to construct the sequence of surrogate variables $\{\hat{\mathbf{X}}^t\}_{t \geq 0}$ with the mentioned properties as desired. To this end, we are inspired by the idea of nonlinear gossiping [34] which splits an exact (projection) operator into multiple small steps of nonlinear operations, while running in parallel with the main recursion; also see [29], [30] for related ideas. In particular, we shall construct the surrogate variables using a recursion that tracks $\{\mathbf{X}^t\}_{t \geq 0}$ and runs in parallel with (14). Meanwhile, the design of this recursion should be bandwidth constrained such that it has to be implementable using compression.

The bandwidth constraint forbids us from setting $\hat{\mathbf{X}}^t = \mathbf{X}^t$ directly. Instead, we only transmit compressed data between agents. As an illustrative example, consider the randomized quantization operator [37]:

$$\text{qsgd}_s(\mathbf{x}; \xi_{q_i}) = \frac{\|\mathbf{x}\|}{s\tau} \cdot \text{sign}(\mathbf{x}) \odot \left[s \frac{|\mathbf{x}|}{\|\mathbf{x}\|} + \xi_{q_i} \right], \quad (15)$$

where \odot denotes element-wise product, $s > 0$ is the number of precision levels, $\tau = 1 + \min\{d/s^2, \sqrt{d}/s\}$ is a scaling factor and $\xi_{q_i} \sim \mathcal{U}[0, 1]^d$ represents the dithering noise. Notice that $\text{qsgd}_s(\cdot)$ can be implemented with an *encoder-decoder* architecture. On the transmitter's side, the *encoder* compresses the d -dimensional input vector into a $d \log_2 s$ -bits string alongside with the norm of vector $\|\mathbf{x}\|$. On the receiver's side, a *decoder* converts the received bits into a quantized real vector in (15). There are also a number of alternatives to the compressors like (15) – including sparsifier that takes the top/random subset of coordinates from $\{1, \dots, d\}$ [24], adaptive quantizer whose precision can be adjusted according to the input messages $\|\mathbf{x}\|$ [32], etc.

¹We have absorbed the term related to $\mathbf{B}(\xi_a)$ into $\tilde{\alpha}$.

We denote $Q : \mathbb{R}^{nd} \times \Omega_q^n \rightarrow \mathbb{R}^{nd}$ as a general compression operator, e.g., the i th block of its output evaluates to $[Q(\mathbf{X}; \xi_q)]_i = \text{qsgd}_s(\mathbf{x}_i; \xi_{q_i})$ when the randomized quantization is used. We assume that these compression operators satisfy the following *noisy and contractive* property:

Assumption III.1. For any fixed $\mathbf{X} \in \mathbb{R}^d$, there exists $\delta \in (0, 1]$ and $\sigma_\xi \geq 0$ such that the output of the compression operator can be decomposed as

$$Q(\mathbf{X}; \xi_q) = \bar{Q}(\mathbf{X}; \bar{\xi}_q) + \mathbf{W}, \quad (16)$$

where $\mathbb{E}[\mathbf{W}] = \mathbf{0}$ and $\mathbb{E}[\|\mathbf{W}\|^2] \leq \sigma_\xi^2$. Moreover,

$$\mathbb{E}_{\bar{\xi}_q} \|\mathbf{X} - \bar{Q}(\mathbf{X}; \bar{\xi}_q)\|^2 \leq (1 - \delta)^2 \|\mathbf{X}\|^2. \quad (17)$$

Note that the above condition is satisfied with common choices of quantizers including (15) and top/random sparsifier. As shown in [24], for (15) it holds with $\delta = \frac{1}{2\tau}$, $\tau = 1 + \min\{d/s^2, \sqrt{d}/s\}$, for top- k sparsifier, it holds with $\delta = k/d$. In (16), \mathbf{W} models the transmission noise when (compressed) messages are sent between agents. For the randomized quantization example in (15), \mathbf{W} may be used to describe the case when the encoded information bits and the real number $\|\mathbf{x}\|$ are transmitted over a noisy channel which introduces zero-mean noise. For adaptive quantization, we also note that a similar condition holds in [32, Definition 3].

Using $Q(\cdot)$, we construct $\hat{\mathbf{X}}^t \approx \mathbf{X}^t$ iteratively by

$$\hat{\mathbf{X}}^t = \hat{\mathbf{X}}^{t-1} + \gamma Q(\mathbf{X}^t - \hat{\mathbf{X}}^{t-1}; \xi_q^t), \quad (18)$$

where $\gamma > 0$ is a stepsize parameter controlling the transmission noise in $\hat{\mathbf{X}}^t$. Notice that when $\mathbf{X}^t = \mathbf{X}$ is constant, the unique fixed point to (18) is where the mean field evaluates to zero given by $\mathbb{E}[Q(\mathbf{X} - \hat{\mathbf{X}}^{t-1}; \xi_q^t)] = \mathbf{0} \Rightarrow \hat{\mathbf{X}}^t = \mathbf{X}$. In this case, the stochastic approximation iteration (18) leads to $\lim_{t \rightarrow \infty} \mathbb{E}[\|\hat{\mathbf{X}}^t - \mathbf{X}\|^2] = \mathcal{O}(\gamma \sigma_\xi^2 / \delta)$. Moreover, setting a time-varying step size of $\gamma_t = \mathcal{O}(1/t)$ leads to a convergence rate of $\mathbb{E}[\|\hat{\mathbf{X}}^t - \mathbf{X}\|^2] = \mathcal{O}(1/t)$.

TiCoPD Algorithm. Observe that (18) converges at a faster rate than the primal-dual update (14). This suggests a *two-timescale simultaneous update* which corresponds to the *upper level* (UL) of (14) and *lower level* (LL) updates of (18). We propose the TiCoPD algorithm as:

$$\begin{cases} \mathbf{X}^{t+1} = \mathbf{X}^t - \alpha (\nabla \mathbf{f}(\mathbf{X}^t; \xi^{t+1}) + \tilde{\boldsymbol{\lambda}}^t + \theta \bar{\mathbf{A}}^\top \bar{\mathbf{A}}(\xi_a^{t+1}) \hat{\mathbf{X}}^t), \\ \tilde{\boldsymbol{\lambda}}^{t+1} = \tilde{\boldsymbol{\lambda}}^t + \eta \bar{\mathbf{A}}^\top \bar{\mathbf{A}}(\xi_a^{t+1}) \hat{\mathbf{X}}^t, \\ \hat{\mathbf{X}}^{t+1} = \hat{\mathbf{X}}^t + \gamma Q(\mathbf{X}^{t+1} - \hat{\mathbf{X}}^t; \xi_q^{t+1}). \end{cases} \quad (19)$$

We observe from (19) that in the UL updates, the i -th local variable $\mathbf{x}_i^t, \tilde{\boldsymbol{\lambda}}_i^t$ requires aggregating the surrogate variables from *active neighbors* $\sum_{j \in \mathcal{N}_i^t} (\hat{\mathbf{x}}_j^t - \hat{\mathbf{x}}_i^t)$. Meanwhile, to incorporate communication compression, the LL updates to the surrogate variable require the *compressed difference* $Q(\mathbf{X}^{t+1} - \hat{\mathbf{X}}^t; \xi_q^{t+1})$ to be transmitted. Accounting for the fact that the neighbor set may vary at each iteration in the time-varying graph setting, this can be achieved by storing a local copy for $\hat{\mathbf{x}}_j^t, \hat{\mathbf{x}}_i^t$ at each neighbor $j \in \mathcal{N}_i$ at agent i , denoted respectively by $\hat{\mathbf{x}}_{i,j}^t, \hat{\mathbf{x}}_{j,i}^t$. We summarize the implementation details in the pseudo code Algorithm 1.

Algorithm 1 TiCoPD Algorithm

- 1: **Input:** Algorithm parameters $\alpha, \theta, \eta, \gamma$, initialization $\mathbf{X}^0, \tilde{\lambda}^0, \hat{\mathbf{x}}_{i,j}^0 = \hat{\mathbf{x}}_j^0, i, j \in [n]$.
 - 2: **for** $t = 0, \dots, T - 1$ **do**
 - 3: Draw a sample for time-varying graph $\xi_a^{t+1} \sim \mathbb{P}_a$.
 - 4: **for** each agent $i \in [n]$ **do**
 - 5: Draw the samples for stochastic gradient $\xi_i^{t+1} \sim \mathbb{P}_i$ and random (noisy) compressor $\xi_{q,i}^{t+1} \sim \mathbb{P}_q$.
 - 6: Receive the compressed differences from $j \in \mathcal{N}_i^t$ of $Q(\mathbf{x}_j^t - \hat{\mathbf{x}}_{i,j}^{t-1}; \xi_{q,j}^t)$ and update

$$\hat{\mathbf{x}}_{i,j}^t = \hat{\mathbf{x}}_{i,j}^{t-1} + \gamma Q(\mathbf{x}_j^t - \hat{\mathbf{x}}_{i,j}^{t-1}; \xi_{q,j}^t), j \in \mathcal{N}_i^t$$
 - Note that the above step is also performed at the transmitter side of $j \in \mathcal{N}_i^t$.
 - 7: Perform the primal-dual update:

$$\mathbf{x}_i^{t+1} = \mathbf{x}_i^t - \alpha(\nabla f_i(\mathbf{x}_i^t; \xi_i^{t+1}) + \tilde{\lambda}_i^t + \theta \sum_{j \in \mathcal{N}_i^t} (\hat{\mathbf{x}}_{j,i}^t - \hat{\mathbf{x}}_{i,j}^t)), \quad (20)$$

$$\tilde{\lambda}_i^{t+1} = \tilde{\lambda}_i^t + \eta \sum_{j \in \mathcal{N}_i^t} (\hat{\mathbf{x}}_{j,i}^t - \hat{\mathbf{x}}_{i,j}^t). \quad (21)$$
 - 8: **end for**
 - 9: **end for**
-

Remark III.2. We conclude the section by remarking about the conceptual differences between TiCoPD and CHOCO-SGD [24]. The latter implements a compressed DSGD algorithm through two steps: adaptation and consensus, i.e.,

$$\begin{aligned} \hat{\mathbf{X}}^{t+1} &= \hat{\mathbf{X}}^t + Q(\mathbf{X}^t - \eta_t \nabla \mathbf{f}(\mathbf{X}^t; \xi^{t+1}) - \hat{\mathbf{X}}^t; \xi_q^{t+1}), \\ \mathbf{X}^{t+1} &= \mathbf{X}^t - \eta_t \nabla \mathbf{f}(\mathbf{X}^t; \xi^{t+1}) + \gamma(\mathbf{W} - \mathbf{I})\hat{\mathbf{X}}^{t+1}. \end{aligned}$$

where \mathbf{W} is doubly stochastic and serves as a weighted adjacency matrix for the static graph G . We observe that CHOCO-SGD is a dynamical consensus modification of CHOCO-GOSSIP in [24]. Particularly, it produces a consensual vector that averages $\mathbf{X}^t - \eta_t \nabla \mathbf{f}(\mathbf{X}^t; \xi^{t+1})$. The design can be easily adapted to algorithms that depend on consensual variables such as gradient tracking, see the recent works [23], [26]. Meanwhile, it is challenging to apply the CHOCO-SGD's recipe on primal-dual algorithms such as (9), (10) where there is no clear 'averaging step' in the algorithm.

The TiCoPD algorithm departed from the CHOCO-SGD's recipe and was derived through a majorization-minimization procedure. As a result, TiCoPD takes the variable $\hat{\mathbf{X}}$ as a surrogate for \mathbf{X} and the involved recursion is a fixed point iteration to achieve $\hat{\mathbf{X}} = \mathbf{X}$. To our best knowledge, TiCoPD is the first algorithm to consider such two timescales update in compressed decentralized optimization.

IV. CONVERGENCE ANALYSIS

This section shows the convergence of the TiCoPD algorithm towards a stationary point of (3) at a sublinear rate. As a preparation, we first define the average decision variable as

$$\bar{\mathbf{x}}^t = \frac{1}{n} \sum_{i=1}^n \mathbf{x}_i^t = \frac{1}{n} (\mathbf{1}^\top \otimes \mathbf{I}_d) \mathbf{X}^t, \quad (22)$$

and using the consensus error operator $\mathbf{K} := (\mathbf{I}_n - \mathbf{1}\mathbf{1}^\top/n) \otimes \mathbf{I}_d$, the consensus error can be expressed as

$$\sum_{i=1}^n \|\mathbf{x}_i^t - \bar{\mathbf{x}}^t\|^2 = \|\mathbf{K}\mathbf{X}^t\|^2 = \|\mathbf{X}^t\|_{\mathbf{K}}^2, \quad (23)$$

and $\bar{\mathbf{Q}} := (\bar{\mathbf{A}}^\top \mathbf{R} \bar{\mathbf{A}})^\dagger$, where $(\cdot)^\dagger$ denotes the Moore-Penrose inverse. From the definitions, we observe that $\bar{\mathbf{A}}^\top \mathbf{R} \bar{\mathbf{A}} \mathbf{K} = \bar{\mathbf{A}}^\top \mathbf{R} \bar{\mathbf{A}} = \mathbf{K} \bar{\mathbf{A}}^\top \mathbf{R} \bar{\mathbf{A}}$ and $\bar{\mathbf{Q}} \bar{\mathbf{A}}^\top \mathbf{R} \bar{\mathbf{A}} = \bar{\mathbf{A}}^\top \mathbf{R} \bar{\mathbf{A}} \bar{\mathbf{Q}} = \mathbf{K}$.

We further make the following standard assumptions about the objective functions and their stochastic gradients.

Assumption IV.1. For any $i \in [n]$, the function f_i is L -smooth such that

$$\|\nabla f_i(\mathbf{x}) - \nabla f_i(\mathbf{y})\| \leq L \|\mathbf{x} - \mathbf{y}\|, \quad \forall \mathbf{x}, \mathbf{y} \in \mathbb{R}^d. \quad (24)$$

There exists $f^* > -\infty$ such that $f_i(\mathbf{x}) \geq f^*$ for any $\mathbf{x} \in \mathbb{R}^d$.

Assumption IV.2. For any $i \in [n]$ and fixed $\mathbf{y} \in \mathbb{R}^d$, there exists $\sigma_i \geq 0$ such that

$$\mathbb{E}[\|\nabla f_i(\mathbf{y}; \xi_i) - \nabla f_i(\mathbf{y})\|^2] \leq \sigma_i^2. \quad (25)$$

Moreover, $\{\xi_i\}_{i=1}^n$ are mutually independent. To simplify notations, we define $\bar{\sigma}^2 = 1/n \sum_{i=1}^n \sigma_i^2$.

Assumption IV.3. There exists constants $\rho_{\max} \geq \rho_{\min} > 0$ and $\tilde{\rho}_{\max} \geq \tilde{\rho}_{\min} > 0$ such that

$$\begin{aligned} \rho_{\min} \mathbf{K} &\preceq \bar{\mathbf{A}}^\top \mathbf{R} \bar{\mathbf{A}} \preceq \rho_{\max} \mathbf{K}, \\ \tilde{\rho}_{\min} \mathbf{K} &\preceq \bar{\mathbf{A}}^\top \bar{\mathbf{A}} \preceq \tilde{\rho}_{\max} \mathbf{K}. \end{aligned} \quad (26)$$

Notice that Assumption IV.3 holds if $\text{diag}(\mathbf{R}) > \mathbf{0}$, i.e. when each edge is selected with a positive probability. Furthermore, as a consequence, it holds $\rho_{\max}^{-1} \mathbf{K} \preceq \bar{\mathbf{Q}} \preceq \rho_{\min}^{-1} \mathbf{K}$.

Assumption IV.4. For any fixed $\mathbf{X} \in \mathbb{R}^{nd}$,

$$\mathbb{E}[\|\bar{\mathbf{A}}^\top \bar{\mathbf{A}}(\xi_a) \mathbf{X} - \bar{\mathbf{A}}^\top \mathbf{R} \bar{\mathbf{A}} \mathbf{X}\|^2] \leq \sigma_A^2 \|\bar{\mathbf{A}} \mathbf{X}\|_{\mathbf{R}}^2. \quad (27)$$

It bounds the variance of $\bar{\mathbf{A}}^\top \bar{\mathbf{A}}(\xi_a) \mathbf{X}$.

The above assumptions guarantee the convergence of TiCoPD algorithm towards a stationary point of (3):

Theorem IV.5. Under Assumptions III.1, IV.1–IV.4, we set the step sizes and parameters as $\theta \geq \theta_{lb}, \alpha \leq \alpha_{ub}, \gamma \leq 1$ where

$$\begin{aligned} \eta &= \frac{\gamma \delta}{8 \tilde{\rho}_{\max}}, \quad \theta_{lb} = \frac{4}{\rho_{\min}} \max \left\{ \frac{2L^2}{na}, \frac{2048 \tilde{\rho}_{\max}}{\gamma \delta \rho_{\min}}, L^2 \right\}, \\ \alpha_{ub} &= \frac{\gamma \delta}{256 \theta} \cdot \min \left\{ \frac{\rho_{\min}^2}{\rho_{\max}^2 \tilde{\rho}_{\max}}, \frac{\rho_{\min}^2}{\sigma_A^2 \rho_{\max} \tilde{\rho}_{\max}}, \right. \\ &\quad \left. \frac{1}{72na \tilde{\rho}_{\max}}, \frac{\rho_{\min}}{2 \tilde{\rho}_{\max} a} \right\}. \end{aligned} \quad (28)$$

Then, for any $T \geq 1$, it holds

$$\begin{aligned} \frac{1}{T} \sum_{t=0}^{T-1} \mathbb{E}[\|\nabla f(\bar{\mathbf{x}}^t)\|^2] &\leq \frac{F_0 - f^*}{\alpha T / 16} + 16 \alpha \omega_\sigma \bar{\sigma}^2 + \frac{128 a \gamma^2 \sigma_\xi^2}{\alpha}, \\ \frac{1}{T} \sum_{t=0}^{T-1} \mathbb{E}[\|\mathbf{X}^t\|_{\mathbf{K}}^2] &\leq \frac{4(F_0 - f^*)}{\alpha \theta \rho_{\min} a T} + \frac{4 \alpha \omega_\sigma}{\theta \rho_{\min} a} \bar{\sigma}^2 + \frac{32 \gamma^2 \sigma_\xi^2}{\alpha \theta \rho_{\min}}, \end{aligned} \quad (29)$$

where $\omega_\sigma = \frac{L}{2n} + a \mathcal{O}(\frac{n}{\gamma \delta})$, $F_0 = f(\bar{\mathbf{x}}^0) + a \mathcal{O}(\|\mathbf{x}^0\|_{\mathbf{K}}^2 + \frac{\alpha}{\eta} \|\tilde{\lambda}^0\|_{\mathbf{K}}^2 + \frac{\alpha}{\eta} \|\nabla \mathbf{f}(\bar{\mathbf{x}}^0)\|_{\mathbf{K}}^2)$. The above statements hold for any $a > 0$, which is a free quantity to be determined.

Note that the constraint on the compressed parameter update stepsize γ is implicit. The complete proof and statement for the theorem can be found in the appendix.

Remark IV.6. We recall from the derivation in Section III that α is implicitly related to $\tilde{\alpha}$. To see that TiCoPD is still a stochastic primal-dual algorithm for the augmented Lagrangian function with $\tilde{\alpha} > 0$ under the step size choices in Theorem IV.5. We note that upon fixing θ , there exists a stepsize $\alpha > 0$ satisfying the parameter choices in the theorem and $\alpha = \frac{1}{\tilde{\alpha} + \theta(M+1)}$, provided that $\tilde{\alpha} > 0$ is sufficiently small.

In the following, we discuss the consequences of Theorem IV.5 through specializing it to various cases and derive the convergence rates of TiCoPD. We shall highlight how choosing the stepsizes α, γ on different timescales under (28) lead to a convergent decentralized algorithm. We concentrate on the setting with a fixed iteration number $T \gg 1$, and define the random variable \mathbb{T} as uniformly and independently drawn from $\{0, 1, \dots, T-1\}$. Particularly, TiCoPD achieves state-of-the-art convergence rates in all settings with unreliable networks. The results are summarized in Table II.

a) *Noiseless Communication* ($\sigma_\xi = 0$): Consider the case when communication channel is noiseless but the communicated messages can be compressed ($\delta > 0$). This is the most common setting considered in the literature, e.g., [25]. Particularly, as the standalone $\hat{\mathbf{X}}$ -update (18) admits linear convergence with $\gamma = 1$, we anticipate that TiCoPD to take a constant γ for optimal performance.

When $\bar{\sigma} > 0$ such that the algorithm takes *noisy gradients*, by selecting $\alpha = \mathcal{O}(\sqrt{n}/(\bar{\sigma}^2 T))$, $\theta = \mathcal{O}(\sqrt{T})$, $\gamma = 1$, $\mathbf{a} = \mathcal{O}(1/\sqrt{T})$, it follows

$$\mathbb{E} \left[\|\nabla f(\bar{\mathbf{x}}^\mathbb{T})\|^2 \right] = \mathcal{O}(\sqrt{\bar{\sigma}^2/(nT)}), \quad (30)$$

and $\mathbb{E} [\|\mathbf{X}^\mathbb{T}\|_{\mathbf{K}}^2] = \mathcal{O}(1/T)$ with $\mathbf{a} = 1$. Observe that with a diminishing α and constant γ , TiCoPD achieves the so-called linear speedup such that its convergence rates are asymptotically equivalent to that of centralized SGD with a minibatch size of n on (3). Moreover, they are comparable to that of decentralized algorithms such as DGD [9] and CHOCO-SGD [25] *without* requiring additional conditions such as bounded gradient heterogeneity.

On the other hand, when $\bar{\sigma} = 0$ such that the algorithm takes *exact gradients*, it is possible to adopt a constant α as well. We have $\theta_{lb} \asymp \delta_1 \asymp \delta^{-1}$, $\alpha_{ub} \asymp \delta^2$, and thus

$$\mathbb{E} \left[\|\nabla f(\bar{\mathbf{x}}^\mathbb{T})\|^2 \right] = \mathcal{O}(1/(\delta^2 T)), \quad \mathbb{E} [\|\mathbf{X}^\mathbb{T}\|_{\mathbf{K}}^2] = \mathcal{O}(1/(\delta T)).$$

Recall that $\delta \in (0, 1]$ of Assumption III.1 is affected by the quality of the compressor. For example, the upper bound on $\mathbb{E} [\|\nabla f(\bar{\mathbf{x}}^\mathbb{T})\|^2]$ evaluates to $\mathcal{O}(ds^{-2}T^{-1})$ for the case of randomized quantization.

b) *Noisy Communication* ($\sigma_\xi > 0$): In this case, we expect the convergence rate to be slower as the algorithm needs to control the communication noise σ_ξ by adopting a decreasing stepsize for γ even in the standalone update (18). This noisy communication setting has only been considered in a small number of works, e.g., [29]–[31].

Noise present?		Convergence Rates of TiCoPD	
Grad. ($\bar{\sigma}$)	Comm. (σ_ξ)	Grad. $\mathbb{E}[\ \nabla f(\bar{\mathbf{x}}^\mathbb{T})\ ^2]$	Cons. $\mathbb{E}[\ \mathbf{X}^\mathbb{T}\ _{\mathbf{K}}^2]$
\times	\times	$\mathcal{O}(1/(\delta^2 T))$	$\mathcal{O}(1/(\delta T))$
\checkmark	\times	$\mathcal{O}(\bar{\sigma}/(n^{\frac{1}{2}} T^{\frac{1}{2}}))$	$\mathcal{O}(1/T)$
\times	\checkmark	$\mathcal{O}((1 + \sigma_\xi^2)/T^{\frac{1}{3}})$	$\mathcal{O}(1/T^{\frac{1}{3}})$
\checkmark	\checkmark	$\mathcal{O}((1 + \sigma_\xi^2)/T^{\frac{1}{3}})$	$\mathcal{O}(1/T^{\frac{1}{3}})$

TABLE II
CONVERGENCE RATES OF TiCoPD ON UNRELIABLE NETWORKS.

With *noisy gradients* ($\bar{\sigma} > 0$), by choosing the step sizes and parameters as $\alpha = \mathcal{O}(T^{-\frac{2}{3}})$, $\theta = \mathcal{O}(T^{\frac{1}{3}})$, $\mathbf{a} = \mathcal{O}(T^{-\frac{1}{3}})$, $\gamma = \mathcal{O}(T^{-\frac{1}{3}})$, it holds

$$\mathbb{E} \left[\|\nabla f(\bar{\mathbf{x}}^\mathbb{T})\|^2 \right] = \mathcal{O} \left(\frac{1 + \sigma_\xi^2}{T^{\frac{1}{3}}} \right), \quad \mathbb{E} [\|\mathbf{X}^\mathbb{T}\|_{\mathbf{K}}^2] = \mathcal{O} \left(\frac{1}{T^{\frac{1}{3}}} \right).$$

We notice that the convergence rates are only at $\mathcal{O}(1/T^{1/3})$ which are slower than the previous case of noiseless communication. That said, when compared to DIMIX [30] which achieves the rate of $\mathcal{O}(T^{-\frac{1}{3}+\epsilon})$, $\epsilon > 0$ for the averaged squared gradient norm, our convergence rate is slightly faster. In addition, the convergence of the DIMIX algorithm requires strong assumptions such as bounded heterogeneity and *a-priori* bounded iterates when used with random- k sparsification and random quantization compressors. The latter restrictions are not found in our results for TiCoPD.

Lastly, we study if *exact gradient* (i.e., $\bar{\sigma} = 0$) may lead to faster convergence. By choosing $\alpha = \mathcal{O}(T^{-\frac{2}{3}})$, $\theta = \mathcal{O}(T^{\frac{1}{3}})$, $\mathbf{a} = \mathcal{O}(T^{-\frac{1}{3}})$, $\gamma = \mathcal{O}(T^{-\frac{1}{3}})$, one only has

$$\mathbb{E} \left[\|\nabla f(\bar{\mathbf{x}}^\mathbb{T})\|^2 \right] = \mathcal{O} \left(\frac{1 + \sigma_\xi^2}{T^{\frac{1}{3}}} \right), \quad \mathbb{E} [\|\mathbf{X}^\mathbb{T}\|_{\mathbf{K}}^2] = \mathcal{O} \left(\frac{1}{T^{\frac{1}{3}}} \right),$$

i.e., similar to the case with noisy gradient.

A. Proof outline of Theorem IV.5

Our plan is to analyze the stable point of TiCoPD through studying the progress of $f(\bar{\mathbf{x}}^t)$ and to control the gradient error by providing an upper bound of $\|\nabla f(\bar{\mathbf{x}}^t)\|^2$. Unlike previous works such as [28], our analysis needs to deal with the surrogate variable $\hat{\mathbf{X}}$ and handle the noise effects in compressed communication. For notational convenience, we denote $\mathbf{v}^t = \alpha \tilde{\lambda}^t + \alpha \nabla f((\mathbf{1}_n \otimes \mathbf{I}_d) \bar{\mathbf{x}}^t)$ as a measure for the tracking performance of the average exact gradient.

The first step is to establish the following descent lemma:

Lemma IV.7. Under Assumption IV.1 and IV.2, when $\alpha \leq \frac{1}{4L}$,

$$\begin{aligned} \mathbb{E} [f(\bar{\mathbf{x}}^{t+1})] &\leq \mathbb{E} [f(\bar{\mathbf{x}}^t)] - \frac{\alpha}{4} \mathbb{E} [\|\nabla f(\bar{\mathbf{x}}^t)\|^2] \\ &\quad + \frac{\alpha L^2}{n} \mathbb{E} [\|\mathbf{X}^t\|_{\mathbf{K}}^2] + \frac{\alpha^2 L}{2n^2} \sum_{i=1}^n \sigma_i^2. \end{aligned} \quad (31)$$

See Appendix A for the proof. Observe that the descent of $\mathbb{E} [f(\bar{\mathbf{x}}^{t+1})]$ depends on the consensus error $\mathbb{E} [\|\mathbf{X}\|_{\mathbf{K}}^2]$ which can be further bounded as:

Lemma IV.8. Under Assumptions IV.1–IV.4 and the step size conditions $\alpha \leq \frac{\rho_{\min}}{16\rho_{\max}\theta} \min\{\frac{1}{\rho_{\max}}, \frac{1}{\sigma_A^2}\}$, $\theta \geq \frac{12L}{\rho_{\min}}$, then

$$\begin{aligned} \mathbb{E} [\|\mathbf{X}^{t+1}\|_{\mathbf{K}}^2] &\leq (1 - (3/2)\alpha\theta\rho_{\min}) \mathbb{E} [\|\mathbf{X}^t\|_{\mathbf{K}}^2] \\ &+ 3\mathbb{E} [\|\mathbf{v}^t\|_{\mathbf{K}}^2] - 2\mathbb{E} [\langle \mathbf{X}^t \mid \mathbf{v}^t \rangle_{(\mathbf{I} - \alpha\theta\bar{\mathbf{A}}^\top \mathbf{R}\bar{\mathbf{A}})\mathbf{K}}] \\ &+ \frac{9\alpha\theta\tilde{\rho}_{\max}^2}{\rho_{\min}} \mathbb{E} [\|\hat{\mathbf{X}}^t - \mathbf{X}^t\|_{\mathbf{K}}^2] + \alpha^2 \sum_{i=1}^n \sigma_i^2. \end{aligned} \quad (32)$$

See Appendix B for the proof. The above lemma reveals that the consensus error $\mathbb{E} [\|\mathbf{X}^t\|_{\mathbf{K}}^2]$ depends on $\mathbb{E} [\|\mathbf{v}^t\|_{\mathbf{K}}^2]$, the weighted inner product between \mathbf{X}^t , \mathbf{v}^t , and the tracking error $\mathbb{E} [\|\hat{\mathbf{X}}^t - \mathbf{X}^t\|_{\mathbf{K}}^2]$. The latter terms admit the following bounds:

Lemma IV.9. Under Assumption IV.1–IV.3 and the step size condition $\alpha \leq 1/4$, for any constant $c > 0$, it follows that

$$\begin{aligned} \mathbb{E} [\|\mathbf{v}^{t+1}\|_{\bar{\mathbf{Q}}+c\mathbf{K}}^2] &\leq (1 + 2\alpha)\mathbb{E} [\|\mathbf{v}^t\|_{\bar{\mathbf{Q}}+c\mathbf{K}}^2] \\ &+ (4\alpha^2\eta^2\tilde{\rho}_{\max}^2 + 6\alpha^3L^4)(\rho_{\min}^{-1} + c)\mathbb{E} [\|\mathbf{X}^t\|_{\mathbf{K}}^2] \\ &+ 2\alpha\eta\mathbb{E} [\langle \mathbf{v}^t \mid \mathbf{X}^t \rangle_{\mathbf{K}+c\bar{\mathbf{A}}^\top \mathbf{R}\bar{\mathbf{A}}}] \\ &+ 2\alpha\eta^2\tilde{\rho}_{\max}^2(\rho_{\min}^{-1} + c)\mathbb{E} [\|\hat{\mathbf{X}}^t - \mathbf{X}^t\|_{\mathbf{K}}^2] \\ &+ 6\alpha^3nL^2(\rho_{\min}^{-1} + c) \left\{ \frac{1}{n^2} \sum_{i=1}^n \sigma_i^2 + \mathbb{E} [\|\nabla f(\bar{\mathbf{x}}^t)\|^2] \right\}. \end{aligned}$$

See Appendix C for the proof.

Lemma IV.10. Under Assumption IV.1–IV.3, and the step size conditions $\alpha \leq \min\{\frac{1}{12}, \frac{\rho_{\min}}{2\rho_{\max}^2\theta}, \frac{\rho_{\min}}{2\sigma_A^2\rho_{\max}\theta}\}$, $\theta \geq \max\{\frac{4L^2}{\rho_{\min}}, \frac{2\eta^2\rho_{\max}^2}{\rho_{\min}}, \eta\}$, it follows that

$$\begin{aligned} \mathbb{E} [\langle \mathbf{X}^{t+1} \mid \mathbf{v}^{t+1} \rangle_{\mathbf{K}}] &\leq \mathbb{E} [\langle \mathbf{X}^t \mid \mathbf{v}^t \rangle_{\mathbf{K} - (\alpha\theta + \alpha\eta)\bar{\mathbf{A}}^\top \mathbf{R}\bar{\mathbf{A}}}] \\ &- \frac{1}{8}\mathbb{E} [\|\mathbf{v}^t\|_{\mathbf{K}}^2] + \frac{3\alpha}{2}\mathbb{E} [\|\mathbf{X}^t\|_{\mathbf{K}}^2] \\ &+ \frac{1}{2}(\alpha\eta^2\rho_{\max}^2 + 5\alpha^2\theta^2\tilde{\rho}_{\max}^2)\mathbb{E} [\|\hat{\mathbf{X}}^t - \mathbf{X}^t\|_{\mathbf{K}}^2] \\ &+ \frac{9}{2}\alpha^3nL^2\mathbb{E} [\|\nabla f(\bar{\mathbf{x}}^t)\|^2] + \left(\frac{9\alpha^3L^2}{2n} + \frac{3\alpha^3}{2}\right) \sum_{i=1}^n \sigma_i^2. \end{aligned}$$

See Appendix D for the proof.

Lemma IV.11. Under Assumptions III.1, IV.2–IV.4 and the step size condition $\alpha \leq \sqrt{\gamma\delta}/(8\rho_{\max}^2\theta^2)$ and $\gamma \leq 1$, then

$$\begin{aligned} \mathbb{E} [\|\hat{\mathbf{X}}^{t+1} - \mathbf{X}^{t+1}\|^2] &\leq (1 - \frac{\gamma\delta}{4})\mathbb{E} [\|\hat{\mathbf{X}}^t - \mathbf{X}^t\|^2] \\ &+ \frac{4}{\gamma\delta}[\alpha^2\theta^2(\rho_{\max}^2 + \sigma_A^2\rho_{\max}/2) + \alpha^2L^2]\mathbb{E} [\|\mathbf{X}^t\|_{\mathbf{K}}^2] \\ &+ \frac{4\alpha\theta}{\gamma\delta}\mathbb{E} [\langle \mathbf{X}^t \mid \mathbf{v}^t \rangle_{\bar{\mathbf{A}}^\top \mathbf{R}\bar{\mathbf{A}}}] + \frac{4}{\gamma\delta}\mathbb{E} [\|\mathbf{v}^t\|_{\mathbf{K}}^2] \\ &+ \frac{4\alpha^2}{\gamma\delta}\mathbb{E} [\|\nabla f(\bar{\mathbf{x}}^t)\|^2] + \frac{2\alpha^2}{\gamma\delta} \sum_{i=1}^n \sigma_i^2 + \gamma^2\sigma_\xi^2. \end{aligned}$$

See Appendix E for the proof. Especially, we remark that the last lemma shows that the effect of communication noise can be controlled by the lower-level step size γ .

To upper bound $\|\nabla f(\bar{\mathbf{x}}^t)\|^2$ alongside the miscellaneous coupling terms, we construct a potential function of the four

error quantities. For some constants $a, b, c, d, e > 0$ to be determined later, we define the potential function F_t as

$$\begin{aligned} F_t &= f(\bar{\mathbf{x}}^t) + a\|\mathbf{X}^t\|_{\mathbf{K}}^2 + b\|\mathbf{v}^t\|_{\bar{\mathbf{Q}}+c\bar{\mathbf{K}}}^2 \\ &+ d\langle \mathbf{X}^t \mid \mathbf{v}^t \rangle_{\bar{\mathbf{K}}} + e\|\hat{\mathbf{X}}^t - \mathbf{X}^t\|^2. \end{aligned} \quad (33)$$

We observe that:

Lemma IV.12. Under Assumptions IV.1–IV.4, III.1. Set

$$\begin{aligned} b &= a \cdot \frac{1}{\alpha\eta}, \quad c = \frac{(\alpha\theta + \alpha\eta)d - 2\alpha\theta a - e\frac{4}{\gamma\delta}\alpha\theta}{2\alpha\eta b}, \\ d &= \frac{1024\tilde{\rho}_{\max}}{\gamma\delta\rho_{\min}}a, \quad e = 8\tilde{\rho}_{\max}\rho_{\min}^{-1}a, \end{aligned} \quad (34)$$

for some $a > 0$. Then, for $\eta = \frac{\gamma\delta}{8\rho_{\max}}$, $\theta \geq \theta_{lb}$, $\alpha \leq \alpha_{ub}$ [cf. (28)], $\gamma \leq 1$, it holds that $F_t \geq f(\bar{\mathbf{x}}^t) \geq f^* > -\infty$, and

$$\begin{aligned} \mathbb{E} [F_{t+1}] &\leq \mathbb{E} [F_t] - \frac{1}{16}\alpha\mathbb{E} [\|\nabla f(\bar{\mathbf{x}}^t)\|^2] \\ &+ \alpha^2\omega_\sigma\bar{\sigma}^2 - \frac{1}{4}\alpha\theta\rho_{\min}a\mathbb{E} [\|\mathbf{X}^t\|_{\mathbf{K}}^2] + 8a\gamma^2\sigma_\xi^2. \end{aligned} \quad (35)$$

such that

$$\omega_\sigma = \frac{L}{2n} + a\left(n + \frac{12L^2}{\eta\rho_{\min}} + \frac{3\rho_{\min}\alpha\theta}{16}(3L^2 + n) + \frac{16n\tilde{\rho}_{\max}}{\gamma\delta\rho_{\min}}\right).$$

The lemma is obtained through satisfying the step size conditions in the previous lemmas. See Appendix F for the proof.

Summing up the inequality (35) from $t = 0$ to $t = T - 1$ and divide both sides by αT gives us

$$\begin{aligned} &\frac{1}{4T} \sum_{t=0}^{T-1} \left\{ \frac{1}{4}\mathbb{E} [\|\nabla f(\bar{\mathbf{x}}^t)\|^2] + \theta\rho_{\min}a\mathbb{E} [\|\mathbf{X}^t\|_{\mathbf{K}}^2] \right\} \\ &\leq \frac{\mathbb{E} [F_0] - \mathbb{E} [F_T]}{\alpha T} + \alpha\omega_\sigma\bar{\sigma}^2 + 8a\frac{\gamma^2\sigma_\xi^2}{\alpha}. \end{aligned} \quad (36)$$

Reshuffling terms yields the conclusions of the theorem.

V. NUMERICAL EXPERIMENTS

This section demonstrates the effectiveness of TiCoPD on practical problems through numerical experiments. As we aim at testing the performance of TiCoPD in unreliable networks, we also evaluate the *total number of bits transmitted across the network*. For benchmarking purposes, throughout this section, we focus only on decentralized algorithms that support compressed message exchanges. Specifically, we compare CHOCO-SGD [24], DIMIX [30], CP-SGD [27], and FSPDA [28], which support different types of compression operators. The hyperparameters of the tested algorithms are hand tuned via a grid search on the magnitude to achieve the lowest gradient norm $\|\nabla f(\bar{\mathbf{x}}^T)\|^2$ after T iterations.

We consider three types of compression operators $Q(\cdot; \xi_q)$. In addition to random quantization in (15) with $s = 2^4$ levels, top- k (resp. random- k) sparsification keeps the k coordinates with the highest magnitude (resp. chosen uniformly at random). Note that each compressed message with random quantization takes $d(\log_2(s) + 1) + 32$ bits to transmit, while the sparsified message takes $64k$ bits to transmit. Lastly, $G = (V, E)$ is a complete graph with n agents. At each iteration, the TiCoPD, DIMIX, FSPDA algorithms draw a

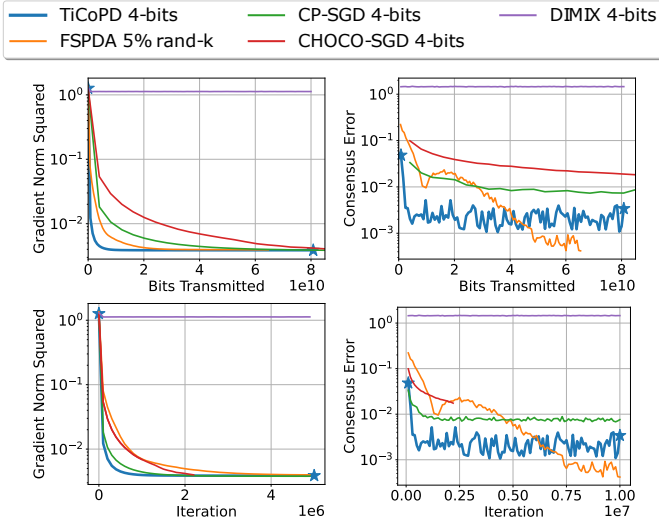


Fig. 1. Convergence rates of compressed algorithms over noiseless communication channel with random edge activation. (Top) against the number of bits transmitted over the network. (Bottom) against the iteration number.

random subgraph $G(\xi_a)$ with only 1 active edge from E , while CHOCO-SGD and CP-SGD take a broadcasting subgraph design where $G(\xi_a)$ is formed by taking the edges incident to only 1 randomly selected agent. Notice that the latter two algorithms are only shown to converge under such restrictive type of time-varying communication graphs [24].

Synthetic Data. Our first set of numerical experiments considers learning a linear model from a synthetic dataset to simulate a controlled decentralized learning environment with heterogeneous data. We consider a set of $n = 10$ agents, where each agent i holds a set of 100 observations $\{\mathbf{z}_{i,j}, \phi(\mathbf{z}_{i,j})\}_{j \in [100]}$. The feature vectors $\mathbf{z}_{i,j} \in \mathbb{R}^{100}$ are generated as $\mathbf{z}_{i,j} \sim \mathcal{N}(\mathbf{m}_i, 0.5\mathbf{I})$, where $\mathbf{m}_i \sim \text{Uniform}\left(\frac{-n/2+i-1}{n/2}, \frac{-n/2+i}{n/2}\right)^{100}$. The labels $\phi(\mathbf{z}_{i,j}) \in [10]$ are determined through the map $\phi(\mathbf{z}) = \arg \max_k \{\mathbf{z}^\top \mathbf{x}_k^{\text{truth}}\}$, where $\mathbf{x}_k^{\text{truth}} \sim \text{Uniform}(-1, 1)^{100}$, $k \in [10]$ is the ground truth model for label k . To learn the linear model $\mathbf{x}^{\text{truth}} = (\mathbf{x}_1^{\text{truth}}, \dots, \mathbf{x}_{10}^{\text{truth}}) \in \mathbb{R}^{1000}$, we consider the local objective function $f_i(\mathbf{x})$ as the sigmoid loss:

$$\sum_{k=1}^{10} \left(\frac{1}{100} \sum_{j=1}^{100} \text{sigmoid}(\mathbb{1}_{\{\phi(\mathbf{z}_{i,j})=k\}} \mathbf{x}_k^\top \mathbf{z}_{i,j}) + \frac{10^{-4}}{2} \|\mathbf{x}_k\|^2 \right),$$

where $\text{sigmoid}(y) = (1 + e^{-y})^{-1}$ for any $y \in \mathbb{R}$ and $\mathbb{1}_{\{\cdot\}} \in \{\pm 1\}$ is the indicator function.

Fig. 1 compares the performance of TiCoPD with benchmarked algorithms when the communication network is *noiseless*, i.e., $\sigma_\xi = 0$. For TiCoPD, we have used $\eta = 0.005, \gamma = 1, \theta = 10^2, \alpha = 10^{-3}$. Notice that algorithms such as CP-SGD achieves similar convergence speed as TiCoPD in terms of the iteration number, yet TiCoPD achieves better communication efficiency as the latter supports computation fully randomized graph topology. Our result corroborates with Theorem IV.5.

We next study the effects of noisy communication channel when $\sigma_\xi = 0.01 > 0$ on the proposed algorithm. Recall from the discussions following Theorem IV.5, the introduction of communication noise may slow down the convergence rate

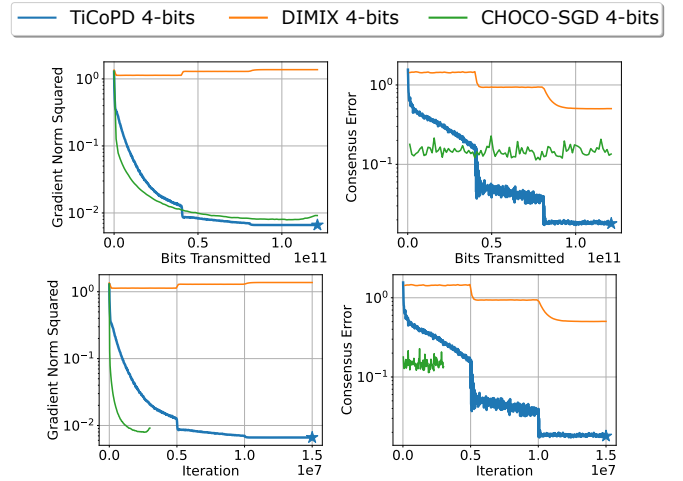


Fig. 2. Convergence rates of compressed algorithms over communication channel with random edge activation and *additive noise*. (Top) against number of bits transmitted over the network. (Bottom) against iteration number.

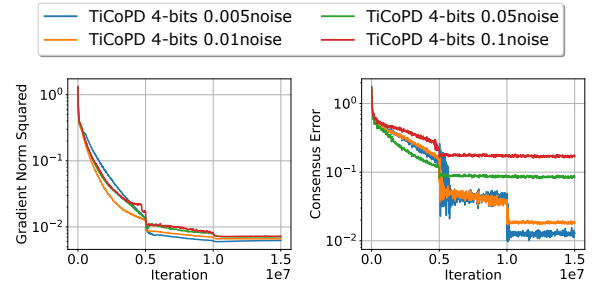


Fig. 3. Convergence rates of TiCoPD over communication channel with random edge activation and different levels of *additive noise*.

of TiCoPD, yet the algorithm can still manage to find a near-stationary and consensual solution of (1). Notice that we adopted a decreasing primal step size for all algorithms where α is reduced by 5 times at every 5×10^6 iterations. For TiCoPD, we set $\gamma = 0.005, \theta = 20, \eta = 6 \times 10^{-6}$, and the initial step size is $\alpha = 5 \times 10^{-5}$.

Fig. 2 compares the convergence behavior of TiCoPD to DIMIX and CHOCO-SGD. We note that under the noisy channel setting, it is not clear if CHOCO-SGD will converge, yet with a carefully tuned stepsize, DIMIX can theoretically converge to a stationary and consensual solution of (1) [30]. From the figure, we observe that TiCoPD converges as predicted by our theorem. Meanwhile, CHOCO-SGD fails to find a consensual solution and DIMIX fails to find a stationary solution. Lastly, Fig. 3 compares the performance of TiCoPD at different levels of communication noise $\sigma_\xi \in \{0.005, 0.01, 0.05, 0.1\}$. As predicted by Theorem IV.5, varying the communication noise level does not affect the convergence rates of TiCoPD, but it affects the magnitude of the dominant term in the stationarity and consensual error of the solutions found.

Real Data. The second set of experiments considers the case of a deep neural network distributed training task. We consider learning a classifier model based on the ResNet-50 architecture (with $d = 2.56 \times 10^9$ parameters) on the ImageNet dataset (with $m = 1,281,168$ samples, split equally to $n = 10$ agents without shuffling). Note that TiCoPD coupled with

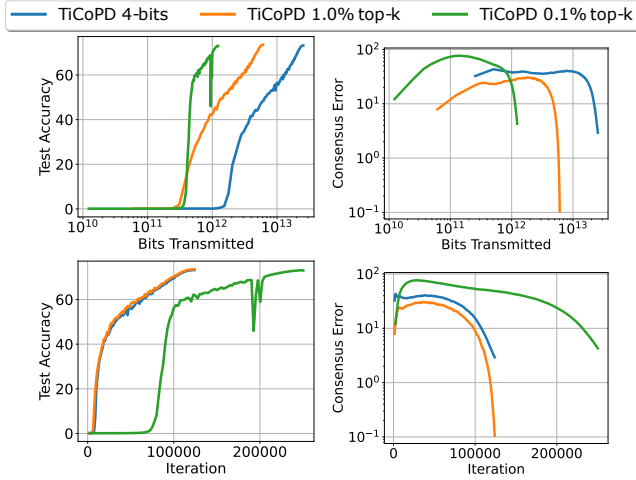


Fig. 4. Training of ResNet-50 model for Imagenet classification. The performance is evaluated on the network-averaged model $\bar{\mathbf{x}}$.

4-bit randomized quantization and 1-edge activated random communication graph offers a communication compression of up to $500\times$ per iteration compared to an uncompressed decentralized algorithm. Further savings can be achieved with a more aggressive compression scheme, e.g., with a 0.1%-sparsifier and 1-edge activated random communication graph. Fig. 4 shows that the TiCoPD converges under such setting as well. As predicted by our Theorem, the network-averaged iterate of TiCoPD will converge to the same degree of error after the transient time, at the cost of only increasing the consensus error.

VI. CONCLUSION

This paper studies a communication efficient primal-dual algorithm for decentralized stochastic optimization with support for time-varying graphs and nonlinear compression schemes such as quantized message exchanges. Our key innovation is to incorporate majorization-minimization and two-timescale updates into the augmented Lagrangian framework. In T iterations, the resultant TiCoPD algorithm finds an $\mathcal{O}(T^{-\frac{1}{2}})$ -stationary solution for smooth (possibly non-convex) problems in the absence of communication noise, and $\mathcal{O}(T^{-\frac{1}{3}})$ -stationary solution in the presence of communication noise. We envisage that the proposed algorithmic framework can inspire the design of sophisticated decentralized algorithms such as algorithms with Nesterov acceleration.

APPENDIX A PROOF OF LEMMA IV.7

As $\mathbf{1}^\top \bar{\mathbf{A}}^\top = \mathbf{0}$, we observe that the updates of $\bar{\mathbf{x}}$ follows the recursion:

$$\bar{\mathbf{x}}^{t+1} = \bar{\mathbf{x}}^t - \frac{\alpha}{n} \mathbf{1}_\otimes^\top \nabla \mathbf{f}(\mathbf{X}^t; \xi^{t+1}), \quad (37)$$

We have denoted the shorthand notations $\mathbf{1}_\otimes^\top := \mathbf{1}^\top \otimes \mathbf{I}$ and $\mathbf{1}_\otimes := \mathbf{1} \otimes \mathbf{I}$. Using Assumption IV.1 and (37), we get

$$\begin{aligned} \mathbb{E} [f(\bar{\mathbf{x}}^{t+1})] &\leq \mathbb{E} \left[f(\bar{\mathbf{x}}^t) - \left\langle \nabla f(\bar{\mathbf{x}}^t) \mid \frac{\alpha}{n} \mathbf{1}_\otimes^\top \nabla \mathbf{f}(\mathbf{X}^t) \right\rangle \right] \\ &+ \frac{L}{2} \mathbb{E} \left[\left\| \frac{\alpha}{n} \mathbf{1}_\otimes^\top \nabla \mathbf{f}(\mathbf{X}^t; \xi^{t+1}) \right\|^2 \right]. \end{aligned} \quad (38)$$

The second term of (38) can be bounded as

$$\begin{aligned} & - \mathbb{E} \left[\left\langle \nabla f(\bar{\mathbf{x}}^t) \mid \frac{\alpha}{n} \mathbf{1}_\otimes^\top \nabla \mathbf{f}(\mathbf{X}^t) \right\rangle \right] \\ & \leq - \frac{\alpha}{2} \mathbb{E} \left[\|\nabla f(\bar{\mathbf{x}}^t)\|^2 \right] + \frac{\alpha}{2n} \mathbb{E} \left[\|\nabla f(\bar{\mathbf{x}}^t) - \mathbf{1}_\otimes^\top \nabla \mathbf{f}(\mathbf{X}^t)\|^2 \right] \\ & \leq - \frac{\alpha}{2} \mathbb{E} \left[\|\nabla f(\bar{\mathbf{x}}^t)\|^2 \right] + \frac{\alpha L^2}{2n} \mathbb{E} \left[\|\mathbf{X}^t\|_{\mathbf{K}}^2 \right]. \end{aligned} \quad (39)$$

By Assumptions IV.1 and IV.2, the third term of (38) can be bounded as

$$\begin{aligned} & \frac{L}{2} \mathbb{E} \left[\left\| \frac{\alpha}{n} \mathbf{1}_\otimes^\top \nabla \mathbf{f}(\mathbf{X}^t; \xi^{t+1}) \right\|^2 \right] \\ & \leq \frac{\alpha^2 L}{2n^2} \sum_{i=1}^n \sigma_i^2 + \frac{\alpha^2 L^3}{n} \mathbb{E} \left[\|\mathbf{X}^t\|_{\mathbf{K}}^2 \right] + \alpha^2 L \mathbb{E} \left[\|\nabla f(\bar{\mathbf{x}}^t)\|^2 \right]. \end{aligned} \quad (40)$$

Combining the above and setting the step size $\alpha \leq \frac{1}{4L}$ concludes the proof of the lemma. \square

APPENDIX B PROOF OF LEMMA IV.8

Define the following quantities:

$$\begin{aligned} \mathbf{e}_s^t &:= \alpha (\nabla \mathbf{f}(\mathbf{X}^t) - \nabla \mathbf{f}(\mathbf{X}^t; \xi_a^{t+1})) \\ &+ \alpha \theta (\bar{\mathbf{A}}^\top \mathbf{R} \bar{\mathbf{A}} - \bar{\mathbf{A}}^\top \bar{\mathbf{A}} (\xi_a^{t+1})) \mathbf{X}^t, \end{aligned} \quad (41)$$

$$\mathbf{e}_g^t := \alpha (\nabla \mathbf{f}(\mathbf{1}_\otimes \bar{\mathbf{x}}^t) - \nabla \mathbf{f}(\mathbf{X}^t)), \quad (42)$$

$$\mathbf{e}_h^t := \alpha \theta \bar{\mathbf{A}}^\top \bar{\mathbf{A}} (\xi_a^{t+1}) (\mathbf{X}^t - \hat{\mathbf{X}}^t), \quad (43)$$

$$\mathbf{v}^t := \alpha \tilde{\lambda}^t + \alpha \nabla \mathbf{f}(\mathbf{1}_\otimes \bar{\mathbf{x}}^t). \quad (44)$$

We notice that

$$\begin{aligned} \mathbf{X}^{t+1} &= \mathbf{X}^t - \alpha (\nabla \mathbf{f}(\mathbf{X}^t; \xi^{t+1}) + \tilde{\lambda}^t + \theta \bar{\mathbf{A}}^\top \bar{\mathbf{A}} (\xi_a^{t+1}) \hat{\mathbf{X}}^t) \\ &= (\mathbf{I} - \alpha \theta \bar{\mathbf{A}}^\top \mathbf{R} \bar{\mathbf{A}}) \mathbf{X}^t - \mathbf{v}^t + \mathbf{e}_s^t + \mathbf{e}_g^t + \mathbf{e}_h^t. \end{aligned} \quad (45)$$

With $\mathbb{E} [\mathbf{e}_s^t | \mathbf{X}^t] = \mathbf{0}$, the consensus error can be measured as

$$\begin{aligned} & \mathbb{E} [\|\mathbf{X}^{t+1}\|_{\mathbf{K}}^2] \\ &= \mathbb{E} \left[\left\| (\mathbf{I} - \alpha \theta \bar{\mathbf{A}}^\top \mathbf{R} \bar{\mathbf{A}}) \mathbf{X}^t - \mathbf{v}^t + \mathbf{e}_s^t + \mathbf{e}_g^t + \mathbf{e}_h^t \right\|_{\mathbf{K}}^2 \right] \\ &\leq \mathbb{E} \left[\left\| (\mathbf{I} - \alpha \theta \bar{\mathbf{A}}^\top \mathbf{R} \bar{\mathbf{A}}) \mathbf{X}^t \right\|_{\mathbf{K}}^2 \right] + \mathbb{E} [\|\mathbf{e}_s^t\|_{\mathbf{K}}^2] \\ &\quad + 3\mathbb{E} [\|\mathbf{e}_g^t\|_{\mathbf{K}}^2] + 3\mathbb{E} [\|\mathbf{e}_h^t\|_{\mathbf{K}}^2] + 3\mathbb{E} [\|\mathbf{v}^t\|_{\mathbf{K}}^2] \\ &\quad - 2\mathbb{E} \left[\left\langle (\mathbf{I} - \alpha \theta \bar{\mathbf{A}}^\top \mathbf{R} \bar{\mathbf{A}}) \mathbf{X}^t \mid \mathbf{v}^t \right\rangle_{\mathbf{K}} \right] \\ &\quad + \frac{\alpha \theta \rho_{\min}}{2} \mathbb{E} \left[\left\langle (\mathbf{I} - \alpha \theta \bar{\mathbf{A}}^\top \mathbf{R} \bar{\mathbf{A}}) \mathbf{X}^t \mid \frac{4}{\alpha \theta \rho_{\min}} (\mathbf{e}_g^t + \mathbf{e}_h^t) \right\rangle_{\mathbf{K}} \right] \\ &\leq (1 + \frac{1}{4} \alpha \theta \rho_{\min}) (1 - 2\alpha \theta \rho_{\min} + \alpha^2 \theta^2 \rho_{\max}^2) \mathbb{E} [\|\mathbf{X}^t\|_{\mathbf{K}}^2] \\ &\quad - 2\mathbb{E} \left[\left\langle \mathbf{X}^t \mid \mathbf{v}^t \right\rangle_{(\mathbf{I} - \alpha \theta \bar{\mathbf{A}}^\top \mathbf{R} \bar{\mathbf{A}}) \mathbf{K}} \right] + (3 + \frac{8}{\alpha \theta \rho_{\min}}) \mathbb{E} [\|\mathbf{e}_g^t\|_{\mathbf{K}}^2] \\ &\quad + (3 + \frac{8}{\alpha \theta \rho_{\min}}) \mathbb{E} [\|\mathbf{e}_h^t\|_{\mathbf{K}}^2] + 3\mathbb{E} [\|\mathbf{v}^t\|_{\mathbf{K}}^2] + \mathbb{E} [\|\mathbf{e}_s^t\|_{\mathbf{K}}^2]. \end{aligned} \quad (46)$$

The error quantities $\mathbb{E} [\|\mathbf{e}_s^t\|_{\mathbf{K}}^2]$, $\mathbb{E} [\|\mathbf{e}_g^t\|_{\mathbf{K}}^2]$, $\mathbb{E} [\|\mathbf{e}_h^t\|_{\mathbf{K}}^2]$ can be simplified as follows. Using the fact that each difference term in \mathbf{e}_s^t has mean zero and are independent when conditioned on \mathbf{X}^t , we obtain

$$\mathbb{E} [\|\mathbf{e}_s^t\|_{\mathbf{K}}^2] \leq \mathbb{E} [\|\mathbf{e}_s^t\|^2]$$

$$\begin{aligned}
&= \mathbb{E} \left[\|\alpha (\nabla \mathbf{f}(\mathbf{X}^t) - \nabla \mathbf{f}(\mathbf{X}^t; \xi^{t+1}))\|^2 \right] \\
&\quad + \mathbb{E} \left[\|\alpha \theta (\bar{\mathbf{A}}^\top \mathbf{R} \bar{\mathbf{A}} - \bar{\mathbf{A}}^\top \bar{\mathbf{A}} (\xi_a^{t+1})) \mathbf{X}^t\|^2 \right] \\
&\stackrel{(25),(27)}{\leq} \alpha^2 \sum_{i=1}^n \sigma_i^2 + \alpha^2 \theta^2 \sigma_A^2 \rho_{\max} \mathbb{E} \left[\|\mathbf{X}^t\|_{\mathbf{K}}^2 \right], \quad (47)
\end{aligned}$$

and

$$\begin{aligned}
\mathbb{E} \left[\|\mathbf{e}_g^t\|_{\mathbf{K}}^2 \right] &\leq \mathbb{E} \left[\|\mathbf{e}_g^t\|^2 \right] \\
&= \alpha^2 \mathbb{E} \left[\|\nabla \mathbf{f}(\mathbf{1}_{\otimes} \bar{\mathbf{x}}^t) - \nabla \mathbf{f}(\mathbf{X}^t)\|^2 \right] \\
&\stackrel{(24)}{\leq} \alpha^2 L^2 \mathbb{E} \left[\|\mathbf{1}_{\otimes} \bar{\mathbf{x}}^t - \mathbf{X}^t\|^2 \right] = \alpha^2 L^2 \mathbb{E} \left[\|\mathbf{X}^t\|_{\mathbf{K}}^2 \right], \quad (48)
\end{aligned}$$

and

$$\begin{aligned}
\mathbb{E} \left[\|\mathbf{e}_h^t\|_{\mathbf{K}}^2 \right] &= \mathbb{E} \left[\left\| \alpha \theta \bar{\mathbf{A}}^\top \bar{\mathbf{A}} (\xi_a^{t+1}) (\hat{\mathbf{X}}^t - \mathbf{X}^t) \right\|_{\mathbf{K}}^2 \right] \\
&\leq \alpha^2 \theta^2 \hat{\rho}_{\max}^2 \mathbb{E} \left[\|\hat{\mathbf{X}}^t - \mathbf{X}^t\|_{\mathbf{K}}^2 \right]. \quad (49)
\end{aligned}$$

Now we simplify the coefficients of the consensus error term by the following step size conditions:

$$\begin{cases} \alpha^2 \theta^2 \rho_{\max}^2 \leq \frac{1}{16} \alpha \theta \rho_{\min} & \Leftrightarrow \alpha \leq \frac{\rho_{\min}}{16 \rho_{\max}^2 \theta}, \\ \alpha^2 \theta^2 \sigma_A^2 \rho_{\max} \leq \frac{1}{16} \alpha \theta \rho_{\min} & \Leftrightarrow \alpha \leq \frac{\rho_{\min}}{16 \sigma_A^2 \rho_{\max} \theta}, \\ 3 \leq \frac{1}{\alpha \theta \rho_{\min}} & \Leftrightarrow \alpha \leq \frac{1}{3 \rho_{\min} \theta}, \\ \frac{9 \alpha L^2}{\theta \rho_{\min}} \leq \frac{1}{16} \alpha \theta \rho_{\min} & \Leftrightarrow \theta \geq \frac{12 L}{\rho_{\min}}. \end{cases} \quad (50)$$

Combining with the upper bounds of $\mathbb{E} \left[\|\mathbf{e}_s^t\|_{\mathbf{K}}^2 \right]$, $\mathbb{E} \left[\|\mathbf{e}_g^t\|_{\mathbf{K}}^2 \right]$, $\mathbb{E} \left[\|\mathbf{e}_h^t\|_{\mathbf{K}}^2 \right]$, the proof is completed. \square

APPENDIX C PROOF OF LEMMA IV.9

Consider expanding \mathbf{v}^{t+1} as

$$\begin{aligned}
\mathbf{v}^{t+1} &\stackrel{(44)}{=} \alpha \tilde{\lambda}^{t+1} + \alpha \nabla \mathbf{f}(\mathbf{1}_{\otimes} \bar{\mathbf{x}}^{t+1}) \\
&= \mathbf{v}^t + \alpha \eta \bar{\mathbf{A}}^\top \bar{\mathbf{A}} (\xi_a^{t+1}) \mathbf{X}^t + \alpha \eta \bar{\mathbf{A}}^\top \bar{\mathbf{A}} (\xi_a^{t+1}) (\hat{\mathbf{X}}^t - \mathbf{X}^t) \\
&\quad + \alpha \nabla \mathbf{f}(\mathbf{1}_{\otimes} \bar{\mathbf{x}}^{t+1}) - \alpha \nabla \mathbf{f}(\mathbf{1}_{\otimes} \bar{\mathbf{x}}^t). \quad (51)
\end{aligned}$$

To simplify notations, denote $\mathcal{N}_v^t := \alpha \eta \bar{\mathbf{A}}^\top \bar{\mathbf{A}} (\xi_a^{t+1}) \mathbf{X}^t + \alpha \eta \bar{\mathbf{A}}^\top \bar{\mathbf{A}} (\xi_a^{t+1}) (\hat{\mathbf{X}}^t - \mathbf{X}^t) + \alpha \nabla \mathbf{f}(\mathbf{1}_{\otimes} \bar{\mathbf{x}}^{t+1}) - \alpha \nabla \mathbf{f}(\mathbf{1}_{\otimes} \bar{\mathbf{x}}^t)$. By Assumption IV.3, for any $\mathbf{y} \in \mathbb{R}^{nd}$ it holds that

$$\mathbb{E} \left[\|\mathbf{y}\|_{\bar{\mathbf{Q}}+\mathbf{c}\mathbf{K}}^2 \right] \leq (\rho_{\min}^{-1} + \mathbf{c}) \mathbb{E} \left[\|\mathbf{y}\|_{\mathbf{K}}^2 \right]. \quad (52)$$

Therefore,

$$\begin{aligned}
\mathbb{E} \left[\|\mathbf{v}^{t+1}\|_{\bar{\mathbf{Q}}+\mathbf{c}\mathbf{K}}^2 \right] &\leq \mathbb{E} \left[\|\mathbf{v}^t\|_{\bar{\mathbf{Q}}+\mathbf{c}\mathbf{K}}^2 \right] + 2 \mathbb{E} \left[\langle \mathbf{v}^t | \mathcal{N}_v^t \rangle_{\bar{\mathbf{Q}}+\mathbf{c}\mathbf{K}} \right] \\
&\quad + 4 \alpha^2 \eta^2 \hat{\rho}_{\max}^2 (\rho_{\min}^{-1} + \mathbf{c}) \left(\mathbb{E} \left[\|\mathbf{X}^t\|_{\mathbf{K}}^2 \right] + \mathbb{E} \left[\|\hat{\mathbf{X}}^t - \mathbf{X}^t\|_{\mathbf{K}}^2 \right] \right) \\
&\quad + 2 \alpha^2 (\rho_{\min}^{-1} + \mathbf{c}) \mathbb{E} \left[\|\nabla \mathbf{f}(\mathbf{1}_{\otimes} \bar{\mathbf{x}}^{t+1}) - \nabla \mathbf{f}(\mathbf{1}_{\otimes} \bar{\mathbf{x}}^t)\|^2 \right]. \quad (53)
\end{aligned}$$

The second term of (53) can be simplified as

$$\begin{aligned}
2 \mathbb{E} \left[\langle \mathbf{v}^t | \mathcal{N}_v^t \rangle_{\bar{\mathbf{Q}}+\mathbf{c}\mathbf{K}} \right] &\leq 2 \alpha \eta \mathbb{E} \left[\langle \mathbf{v}^t | \mathbf{X}^t \rangle_{(\bar{\mathbf{Q}}+\mathbf{c}\mathbf{K}) \bar{\mathbf{A}}^\top \bar{\mathbf{R}} \bar{\mathbf{A}}} \right] \\
&\quad + 2 \alpha \mathbb{E} \left[\|\mathbf{v}^t\|_{\bar{\mathbf{Q}}+\mathbf{c}\mathbf{K}}^2 \right] + \alpha \eta^2 \hat{\rho}_{\max}^2 \mathbb{E} \left[\|\hat{\mathbf{X}}^t - \mathbf{X}^t\|_{\bar{\mathbf{Q}}+\mathbf{c}\mathbf{K}}^2 \right] \\
&\quad + \alpha (\rho_{\min}^{-1} + \mathbf{c}) \mathbb{E} \left[\|\nabla \mathbf{f}(\mathbf{1}_{\otimes} \bar{\mathbf{x}}^{t+1}) - \nabla \mathbf{f}(\mathbf{1}_{\otimes} \bar{\mathbf{x}}^t)\|^2 \right]. \quad (54)
\end{aligned}$$

The proof is concluded by combining the above inequalities with the auxiliary Lemma G.1 (to be shown later) and simplifying $\bar{\mathbf{Q}} \bar{\mathbf{A}}^\top \bar{\mathbf{R}} \bar{\mathbf{A}} = \mathbf{K}$ and $\mathbf{K} \bar{\mathbf{A}}^\top \bar{\mathbf{R}} \bar{\mathbf{A}} = \bar{\mathbf{A}}^\top \bar{\mathbf{R}} \bar{\mathbf{A}}$. \square

APPENDIX D

PROOF OF LEMMA IV.10

We denote $\mathcal{N}_{\mathbf{R}} = \mathbf{I} - \alpha \theta \bar{\mathbf{A}}^\top \bar{\mathbf{R}} \bar{\mathbf{A}}$. By (45) and (51), it holds

$$\begin{aligned}
\mathbb{E} \left[\langle \mathbf{X}^{t+1} | \mathbf{v}^{t+1} \rangle_{\mathbf{K}} \right] &= \mathbb{E} \left[\langle \mathbf{X}^t | \mathbf{v}^t \rangle_{\mathcal{N}_{\mathbf{R}} \mathbf{K} - \alpha \eta \mathbf{K} \bar{\mathbf{A}}^\top \bar{\mathbf{R}} \bar{\mathbf{A}}} \right] \\
&\quad + \alpha \eta \mathbb{E} \left[\|\mathbf{X}^t\|_{\mathcal{N}_{\mathbf{R}} \mathbf{K} \bar{\mathbf{A}}^\top \bar{\mathbf{R}} \bar{\mathbf{A}}}^2 \right] - \mathbb{E} \left[\|\mathbf{v}^t\|_{\mathbf{K}}^2 \right] \\
&\quad + \alpha \mathbb{E} \left[\langle \mathbf{X}^t | \nabla \mathbf{f}(\mathbf{1}_{\otimes} \bar{\mathbf{x}}^{t+1}) - \nabla \mathbf{f}(\mathbf{1}_{\otimes} \bar{\mathbf{x}}^t) \rangle_{\mathcal{N}_{\mathbf{R}} \mathbf{K}} \right] \\
&\quad - \alpha \mathbb{E} \left[\langle \mathbf{v}^t | \nabla \mathbf{f}(\mathbf{1}_{\otimes} \bar{\mathbf{x}}^{t+1}) - \nabla \mathbf{f}(\mathbf{1}_{\otimes} \bar{\mathbf{x}}^t) \rangle_{\mathbf{K}} \right] \\
&\quad - \mathbb{E} \left[\langle \mathcal{N}_{\mathbf{R}} \mathbf{X}^t - \mathbf{v}^t | \frac{\eta}{\theta} \mathbf{e}_h^t \rangle_{\mathbf{K}} \right] \\
&\quad + \mathbb{E} \left[\langle \mathbf{e}_g^t + \mathbf{e}_h^t | \mathbf{v}^t + \alpha \eta \bar{\mathbf{A}}^\top \bar{\mathbf{R}} \bar{\mathbf{A}} \mathbf{X}^t - \frac{\eta}{\theta} \mathbf{e}_h^t \rangle_{\mathbf{K}} \right] \\
&\quad + \alpha \mathbb{E} \left[\langle \mathbf{e}_s^t + \mathbf{e}_g^t + \mathbf{e}_h^t | \nabla \mathbf{f}(\mathbf{1}_{\otimes} \bar{\mathbf{x}}^{t+1}) - \nabla \mathbf{f}(\mathbf{1}_{\otimes} \bar{\mathbf{x}}^t) \rangle_{\mathbf{K}} \right]. \quad (55)
\end{aligned}$$

Now notice that by applying Young's inequality on the fourth to eighth terms of the above, we get

$$\begin{aligned}
&\alpha \mathbb{E} \left[\langle \mathbf{X}^t | \nabla \mathbf{f}(\mathbf{1}_{\otimes} \bar{\mathbf{x}}^{t+1}) - \nabla \mathbf{f}(\mathbf{1}_{\otimes} \bar{\mathbf{x}}^t) \rangle_{\mathcal{N}_{\mathbf{R}} \mathbf{K}} \right] \\
&\leq \frac{\alpha}{2} \mathbb{E} \left[\|\mathbf{I} - \alpha \theta \bar{\mathbf{A}}^\top \bar{\mathbf{R}} \bar{\mathbf{A}}\|_{\mathbf{K}}^2 \right] \\
&\quad + \frac{\alpha}{2} \mathbb{E} \left[\|\nabla \mathbf{f}(\mathbf{1}_{\otimes} \bar{\mathbf{x}}^{t+1}) - \nabla \mathbf{f}(\mathbf{1}_{\otimes} \bar{\mathbf{x}}^t)\|^2 \right],
\end{aligned}$$

and

$$\begin{aligned}
&-\alpha \mathbb{E} \left[\langle \mathbf{v}^t | \nabla \mathbf{f}(\mathbf{1}_{\otimes} \bar{\mathbf{x}}^{t+1}) - \nabla \mathbf{f}(\mathbf{1}_{\otimes} \bar{\mathbf{x}}^t) \rangle_{\mathbf{K}} \right] \\
&\leq \frac{\alpha}{2} \mathbb{E} \left[\|\mathbf{v}^t\|_{\mathbf{K}}^2 \right] + \frac{\alpha}{2} \mathbb{E} \left[\|\nabla \mathbf{f}(\mathbf{1}_{\otimes} \bar{\mathbf{x}}^{t+1}) - \nabla \mathbf{f}(\mathbf{1}_{\otimes} \bar{\mathbf{x}}^t)\|^2 \right],
\end{aligned}$$

and

$$\begin{aligned}
&-\alpha \mathbb{E} \left[\langle \mathcal{N}_{\mathbf{R}} \mathbf{X}^t - \mathbf{v}^t | \eta \bar{\mathbf{A}}^\top \bar{\mathbf{A}} (\xi_a^{t+1}) (\hat{\mathbf{X}}^t - \mathbf{X}^t) \rangle_{\mathbf{K}} \right] \\
&\leq \alpha \mathbb{E} \left[\|\mathbf{I} - \alpha \theta \bar{\mathbf{A}}^\top \bar{\mathbf{R}} \bar{\mathbf{A}}\|_{\mathbf{K}}^2 \right] + \alpha \mathbb{E} \left[\|\mathbf{v}^t\|_{\mathbf{K}}^2 \right] \\
&\quad + \frac{\alpha \eta^2 \hat{\rho}_{\max}^2}{2} \mathbb{E} \left[\|\hat{\mathbf{X}}^t - \mathbf{X}^t\|_{\mathbf{K}}^2 \right],
\end{aligned}$$

and

$$\begin{aligned}
&\mathbb{E} \left[\langle \mathbf{e}_g^t + \mathbf{e}_h^t | \mathbf{v}^t + \alpha \eta \bar{\mathbf{A}}^\top \bar{\mathbf{R}} \bar{\mathbf{A}} \mathbf{X}^t - \frac{\eta}{\theta} \mathbf{e}_h^t \rangle_{\mathbf{K}} \right] \\
&\quad + \alpha \mathbb{E} \left[\langle \mathbf{e}_s^t + \mathbf{e}_g^t + \mathbf{e}_h^t | \nabla \mathbf{f}(\mathbf{1}_{\otimes} \bar{\mathbf{x}}^{t+1}) - \nabla \mathbf{f}(\mathbf{1}_{\otimes} \bar{\mathbf{x}}^t) \rangle_{\mathbf{K}} \right] \\
&\leq \frac{3\alpha}{2} \mathbb{E} \left[\|\mathbf{e}_s^t\|_{\mathbf{K}}^2 \right] + \left(1 + \frac{1}{2} + \frac{3\alpha}{2}\right) \mathbb{E} \left[\|\mathbf{e}_g^t\|_{\mathbf{K}}^2 \right] \\
&\quad + \left(1 + \frac{\eta^2}{2\theta^2} - \frac{\eta}{\theta} + \frac{3\alpha}{2}\right) \mathbb{E} \left[\|\mathbf{e}_h^t\|_{\mathbf{K}}^2 \right] \\
&\quad + \frac{1}{2} \left(1 + \frac{1}{2}\right) \mathbb{E} \left[\|\mathbf{v}^t\|_{\mathbf{K}}^2 \right] + \frac{1}{2} (1+2) \alpha^2 \eta^2 \mathbb{E} \left[\|\bar{\mathbf{A}}^\top \bar{\mathbf{R}} \bar{\mathbf{A}} \mathbf{X}^t\|_{\mathbf{K}}^2 \right] \\
&\quad + \frac{\alpha}{2} \mathbb{E} \left[\|\nabla \mathbf{f}(\mathbf{1}_{\otimes} \bar{\mathbf{x}}^{t+1}) - \nabla \mathbf{f}(\mathbf{1}_{\otimes} \bar{\mathbf{x}}^t)\|_{\mathbf{K}}^2 \right].
\end{aligned}$$

By the step size conditions $\alpha \leq 1$ and $\eta \leq \theta$, we can combine the above inequalities to get

$$\begin{aligned}
&\mathbb{E} \left[\langle \mathbf{X}^{t+1} | \mathbf{v}^{t+1} \rangle_{\mathbf{K}} \right] \\
&\leq \mathbb{E} \left[\langle \mathbf{X}^t | \mathbf{v}^t \rangle_{\mathbf{K} - (\alpha \theta + \alpha \eta) \bar{\mathbf{A}}^\top \bar{\mathbf{R}} \bar{\mathbf{A}}} \right] + \left(\frac{3\alpha}{2} - \frac{1}{4} \right) \mathbb{E} \left[\|\mathbf{v}^t\|_{\mathbf{K}}^2 \right]
\end{aligned}$$

$$\begin{aligned}
& + \frac{3\alpha}{2}(1 - 2\alpha\theta\rho_{\min} + \alpha^2\theta^2\rho_{\max}^2 + \alpha\eta^2\rho_{\max}^2)\mathbb{E}[\|\mathbf{X}^t\|_{\mathbf{K}}^2] \\
& + \frac{\alpha\eta^2\rho_{\max}^2}{2}\mathbb{E}[\|\hat{\mathbf{X}}^t - \mathbf{X}^t\|_{\mathbf{K}}^2] \\
& + \frac{3\alpha}{2}\mathbb{E}[\|\nabla\mathbf{f}(\mathbf{1}_{\otimes}\bar{\mathbf{x}}^{t+1}) - \nabla\mathbf{f}(\mathbf{1}_{\otimes}\bar{\mathbf{x}}^t)\|_{\mathbf{K}}^2] \\
& + \frac{3\alpha}{2}\mathbb{E}[\|\mathbf{e}_s^t\|_{\mathbf{K}}^2] + 3\mathbb{E}[\|\mathbf{e}_g^t\|_{\mathbf{K}}^2] + \frac{5}{2}\mathbb{E}[\|\mathbf{e}_h^t\|_{\mathbf{K}}^2].
\end{aligned}$$

Now apply the inequalities in (47), (48) (49) to see that

$$\begin{aligned}
& \mathbb{E}[\langle \mathbf{X}^{t+1} | \mathbf{v}^{t+1} \rangle_{\mathbf{K}}] \\
& \leq \mathbb{E}[\langle \mathbf{X}^t | \mathbf{v}^t \rangle_{\mathbf{K} - (\alpha\theta + \alpha\eta)\bar{\mathbf{A}}^\top\mathbf{R}\bar{\mathbf{A}}} + (\frac{3\alpha}{2} - \frac{1}{4})\mathbb{E}[\|\mathbf{v}^t\|_{\mathbf{K}}^2] \\
& \quad + \frac{3\alpha}{2}(1 - 2\alpha\theta\rho_{\min} + \alpha^2\theta^2\rho_{\max}^2 + \alpha\eta^2\rho_{\max}^2 \\
& \quad + \alpha^2\theta^2\sigma_A^2\rho_{\max} + 2\alpha L^2)\mathbb{E}[\|\mathbf{X}^t\|_{\mathbf{K}}^2] \\
& \quad + \frac{1}{2}(\alpha\eta^2\rho_{\max}^2 + 5\alpha^2\theta^2\tilde{\rho}_{\max}^2)\mathbb{E}[\|\hat{\mathbf{X}}^t - \mathbf{X}^t\|_{\mathbf{K}}^2] \\
& \quad + \frac{3\alpha}{2}\mathbb{E}[\|\nabla\mathbf{f}(\mathbf{1}_{\otimes}\bar{\mathbf{x}}^{t+1}) - \nabla\mathbf{f}(\mathbf{1}_{\otimes}\bar{\mathbf{x}}^t)\|_{\mathbf{K}}^2] + \frac{3\alpha^3}{2}\sum_{i=1}^n\sigma_i^2.
\end{aligned} \tag{56}$$

Then, under the following step size conditions:

$$\begin{cases}
\alpha^2\theta^2\rho_{\max}^2 \leq \alpha\theta\rho_{\min}/2 & \Leftrightarrow \alpha \leq \frac{\rho_{\min}}{2\rho_{\max}^2\theta}, \\
\alpha\eta^2\rho_{\max}^2 \leq \alpha\theta\rho_{\min}/2 & \Leftrightarrow \theta \geq \frac{2\eta^2\rho_{\max}^2}{\rho_{\min}}, \\
\alpha^2\theta^2\sigma_A^2\rho_{\max} \leq \alpha\theta\rho_{\min}/2 & \Leftrightarrow \alpha \leq \frac{\rho_{\min}}{2\sigma_A^2\rho_{\max}\theta}, \\
2\alpha L^2 \leq \alpha\theta\rho_{\min}/2 & \Leftrightarrow \theta \geq 4L^2/\rho_{\min},
\end{cases} \tag{57}$$

and $\alpha \leq 1/12$, the proof is completed by applying the result of Lemma G.1. \square

APPENDIX E PROOF OF LEMMA IV.11

By Assumption III.1, it holds that

$$\begin{aligned}
& \mathbb{E}[\|\hat{\mathbf{X}}^{t+1} - \mathbf{X}^{t+1}\|^2] \\
& = \mathbb{E}[\|\hat{\mathbf{X}}^t - \mathbf{X}^{t+1} + \gamma Q(\mathbf{X}^{t+1} - \hat{\mathbf{X}}^t; \xi_q^{t+1})\|^2] \\
& \leq (1 - \gamma\delta)\mathbb{E}[\|\mathbf{X}^{t+1} - \mathbf{X}^t + \mathbf{X}^t - \hat{\mathbf{X}}^t\|^2] + \gamma^2\sigma_\xi^2 \\
& \leq (1 - \gamma\delta)(1 + \frac{1}{\tau})\mathbb{E}[\|\mathbf{X}^t - \hat{\mathbf{X}}^t\|^2] \\
& \quad + (1 - \gamma\delta)(1 + \tau)\mathbb{E}[\|\mathbf{X}^{t+1} - \mathbf{X}^t\|^2] + \gamma^2\sigma_\xi^2 \\
& \leq (1 - \frac{\gamma\delta}{2})\mathbb{E}[\|\mathbf{X}^t - \hat{\mathbf{X}}^t\|^2] + (\frac{2}{\gamma\delta} - 2)\mathbb{E}[\|\mathbf{X}^{t+1} - \mathbf{X}^t\|^2] \\
& \quad + \gamma^2\sigma_\xi^2,
\end{aligned} \tag{58}$$

where the last inequality is obtained by choosing $\tau = \frac{1-\gamma\delta}{\gamma\delta/2}$. By (45), we get

$$\begin{aligned}
& \mathbb{E}[\|\mathbf{X}^{t+1} - \mathbf{X}^t\|^2] \\
& \leq 2\alpha^2\theta^2\mathbb{E}[\|\bar{\mathbf{A}}^\top\mathbf{R}\bar{\mathbf{A}}\mathbf{X}^t\|^2] + 2\alpha\theta\mathbb{E}[\langle \mathbf{X}^t | \mathbf{v}^t \rangle_{\bar{\mathbf{A}}^\top\mathbf{R}\bar{\mathbf{A}}\mathbf{K}}] \\
& \quad + 2\mathbb{E}[\|\mathbf{v}^t\|^2] + 2\mathbb{E}[\|\mathbf{e}_g^t\|^2] + 2\mathbb{E}[\|\mathbf{e}_h^t\|^2] + \mathbb{E}[\|\mathbf{e}_s^t\|^2] \\
& \leq (2\alpha^2\theta^2\rho_{\max}^2 + 2\alpha^2L^2 + \alpha^2\theta^2\sigma_A^2\rho_{\max})\mathbb{E}[\|\mathbf{X}^t\|_{\mathbf{K}}^2] \\
& \quad + 2\alpha\theta\mathbb{E}[\langle \mathbf{X}^t | \mathbf{v}^t \rangle_{\bar{\mathbf{A}}^\top\mathbf{R}\bar{\mathbf{A}}} + 2\mathbb{E}[\|\mathbf{v}^t\|^2]
\end{aligned}$$

$$+ 2\alpha^2\theta^2\tilde{\rho}_{\max}^2\mathbb{E}[\|\hat{\mathbf{X}}^t - \mathbf{X}^t\|^2] + \alpha^2\sum_{i=1}^n\sigma_i^2,$$

where the last inequality is due to (47), (48) (49). By the fact that $\tilde{\lambda}^t = \bar{\mathbf{A}}^\top\lambda^t \Rightarrow (\mathbf{1} \otimes \mathbf{I}_d)^\top\tilde{\lambda}^t = 0$, we have

$$\begin{aligned}
\|\mathbf{v}^t\|_{\mathbf{K}}^2 & = \|\alpha\tilde{\lambda}^t + \alpha\nabla\mathbf{f}(\mathbf{1}_{\otimes}\bar{\mathbf{x}}^t)\|_{(\mathbf{I} - \frac{1}{n}\mathbf{1}\mathbf{1}^\top) \otimes \mathbf{I}_d}^2 \\
& = \|\mathbf{v}^t\|^2 - \alpha^2\|\nabla\mathbf{f}(\mathbf{1}_{\otimes}\bar{\mathbf{x}}^t)\|_{\frac{1}{n}\mathbf{1}\mathbf{1}^\top \otimes \mathbf{I}_d}^2 \\
& = \|\mathbf{v}^t\|^2 - \alpha^2\|\nabla f(\bar{\mathbf{x}}^t)\|^2.
\end{aligned} \tag{59}$$

Combining the above and applying $2\alpha^2\theta^2\tilde{\rho}_{\max}^2 \leq \gamma\delta/4 \Leftrightarrow \alpha \leq \sqrt{\gamma\delta/(8\tilde{\rho}_{\max}^2\theta^2)}$ completes the proof. \square

APPENDIX F PROOF OF LEMMA IV.12

We first obtain a lower bound for F_t . By the inequality $|\langle \mathbf{x} | \mathbf{y} \rangle| \leq \frac{1}{2\delta_0}\|\mathbf{x}\|^2 + \frac{\delta_0}{2}\|\mathbf{y}\|^2$ for any $\delta_0 > 0$,

$$\begin{aligned}
F_t & \geq f(\bar{\mathbf{x}}^t) + \mathbf{a}\|\mathbf{X}^t\|_{\mathbf{K}}^2 + \|\mathbf{v}^t\|_{\mathbf{b}\bar{\mathbf{Q}} + \mathbf{b}\mathbf{c}\mathbf{K}}^2 - \frac{\mathbf{d}}{2\delta_0}\|\mathbf{X}^t\|_{\mathbf{K}}^2 \\
& \quad - \frac{\mathbf{d}\delta_0}{2}\|\mathbf{v}^t\|_{\mathbf{K}}^2 + \mathbf{e}\|\hat{\mathbf{X}}^t - \mathbf{X}^t\|^2 \\
& = f(\bar{\mathbf{x}}^t) + (\mathbf{a} - \frac{\mathbf{d}}{2\delta_0})\|\mathbf{X}^t\|_{\mathbf{K}}^2 + \|\mathbf{v}^t\|_{\mathbf{b}\bar{\mathbf{Q}} + (\mathbf{b}\mathbf{c} - \mathbf{d}\delta_0/2)\mathbf{K}}^2 \\
& \quad + \mathbf{e}\|\hat{\mathbf{X}}^t - \mathbf{X}^t\|^2 \\
& \stackrel{(\delta_0 = \frac{\mathbf{d}}{2\mathbf{a}})}{\geq} f(\bar{\mathbf{x}}^t) + \|\mathbf{v}^t\|_{\mathbf{b}\bar{\mathbf{Q}} + (\mathbf{b}\mathbf{c} - \frac{\mathbf{d}^2}{4\mathbf{a}})\mathbf{K}}^2 + \mathbf{e}\|\hat{\mathbf{X}}^t - \mathbf{X}^t\|^2 \\
& \stackrel{(26)}{\geq} f(\bar{\mathbf{x}}^t) + \|\mathbf{v}^t\|_{(\mathbf{b}\cdot\tilde{\rho}_{\max}^{-1} + \mathbf{b}\mathbf{c} - \frac{\mathbf{d}^2}{4\mathbf{a}})\mathbf{K}}^2 + \mathbf{e}\|\hat{\mathbf{X}}^t - \mathbf{X}^t\|^2.
\end{aligned} \tag{60}$$

To simplify notation, we set $\delta_1 = \frac{1024\tilde{\rho}_{\max}}{\gamma\delta\rho_{\min}}$, $\delta_2 = 8\tilde{\rho}_{\max}\rho_{\min}^{-1}$ in this section, i.e. $\mathbf{d} = \delta_1\mathbf{a}$, $\mathbf{e} = \delta_2\mathbf{a}$. By choosing $\delta_1 \geq 2\delta_2 + 2$, $\alpha \leq \frac{4}{\eta\tilde{\rho}_{\max}\delta_1^2}$, it holds

$$\begin{aligned}
& \mathbf{b} \cdot \tilde{\rho}_{\max}^{-1} + \mathbf{b}\mathbf{c} - \frac{\mathbf{d}^2}{4\mathbf{a}} \\
& = \mathbf{a} \left(\frac{1}{\alpha\eta\tilde{\rho}_{\max}} + \alpha(\frac{\delta_1}{2}(\theta + \eta) - \theta) - \delta_2\alpha\theta - \frac{\delta_1^2}{4} \right) \geq 0.
\end{aligned} \tag{61}$$

Therefore, $F_t \geq f(\bar{\mathbf{x}}^t) \geq f^* > -\infty$. If the parameters are chosen according to (34), then

$$\begin{aligned}
\mathbf{W}_{xv} & = -\mathbf{a} \cdot 2\mathbf{K} + \mathbf{a} \cdot 2\alpha\theta\bar{\mathbf{A}}^\top\mathbf{R}\bar{\mathbf{A}} + \mathbf{b} \cdot 2\alpha\eta(\mathbf{K} + \mathbf{c}\bar{\mathbf{A}}^\top\mathbf{R}\bar{\mathbf{A}}) \\
& \quad - \mathbf{d} \cdot (\alpha\theta + \alpha\eta)\bar{\mathbf{A}}^\top\mathbf{R}\bar{\mathbf{A}} + \mathbf{e} \frac{4\alpha\theta}{\gamma\delta}\bar{\mathbf{A}}^\top\mathbf{R}\bar{\mathbf{A}} = 0,
\end{aligned} \tag{62}$$

and the inner product term in (33) vanishes. Consider the iterative relationship of the potential function. Combining the previous lemma, we can obtain

$$\begin{aligned}
\mathbb{E}[F_{t+1}] & \leq \mathbb{E}[F_t] + \bar{\omega}_f\mathbb{E}[\|\nabla f(\bar{\mathbf{x}}^t)\|^2] + \alpha^2\bar{\omega}_\sigma\bar{\sigma}^2 \\
& \quad + \bar{\omega}_x\mathbb{E}[\|\mathbf{X}^t\|_{\mathbf{K}}^2] + \bar{\omega}_v\mathbb{E}[\|\mathbf{v}^t\|_{\mathbf{K}}^2] + 8\alpha\gamma^2\sigma_\xi^2 \\
& \quad + \bar{\omega}_{\hat{\mathbf{x}}}\mathbb{E}[\|\hat{\mathbf{X}}^t - \mathbf{X}^t\|^2] + \mathbb{E}[\langle \mathbf{X}^t | \mathbf{v}^t \rangle_{\mathbf{W}_{xv}}],
\end{aligned} \tag{63}$$

where the coefficients are given by

$$\begin{aligned}
\bar{\omega}_f & = -\frac{\alpha}{4} + \mathbf{b} \cdot 6\alpha^3(\rho_{\min}^{-1} + \mathbf{c})nL^2 + \mathbf{d} \cdot \frac{9}{2}\alpha^3nL^2 \\
& \quad + \mathbf{e} \cdot \frac{4}{\gamma\delta}\alpha^2,
\end{aligned} \tag{64}$$

and

$$\begin{aligned} \bar{\omega}_x &= \frac{\alpha L^2}{n} - \mathbf{a} \cdot \frac{3}{2} \alpha \theta \rho_{\min} \\ &+ \mathbf{b} \cdot (4\alpha^2 \eta^2 \tilde{\rho}_{\max}^2 + 6\alpha^3 L^4) (\rho_{\min}^{-1} + \mathbf{c}) + \mathbf{d} \cdot \frac{3\alpha}{2} \\ &+ \mathbf{e} \cdot \frac{4}{\gamma \delta} [\alpha^2 \theta^2 (\rho_{\max}^2 + \sigma_A^2 \rho_{\max}/2) + \alpha^2 L^2], \end{aligned} \quad (65)$$

and

$$\bar{\omega}_v = \mathbf{a} \cdot 3 + \mathbf{b} \cdot 2\alpha (\rho_{\min}^{-1} + \mathbf{c}) - \mathbf{d} \cdot \frac{1}{8} + \mathbf{e} \cdot \frac{4}{\gamma \delta}, \quad (66)$$

and

$$\begin{aligned} \bar{\omega}_{\hat{x}} &= \mathbf{a} \cdot 9\alpha \theta \tilde{\rho}_{\max}^2 \rho_{\min}^{-1} + \mathbf{b} \cdot 2\alpha \eta^2 \tilde{\rho}_{\max}^2 (\rho_{\min}^{-1} + \mathbf{c}) \\ &+ \mathbf{d} \cdot \frac{1}{2} (\alpha \eta^2 \rho_{\max}^2 + 5\alpha^2 \theta^2 \tilde{\rho}_{\max}^2) + \mathbf{e} \cdot -\frac{\gamma \delta}{4}, \end{aligned} \quad (67)$$

and

$$\begin{aligned} \bar{\omega}_\sigma &= \frac{L}{2n} + \mathbf{a}n + \mathbf{b} \cdot 6\alpha (\rho_{\min}^{-1} + \mathbf{c})L^2 + \mathbf{d} \cdot \left(\frac{9\alpha L^2}{2} + \frac{3\alpha n}{2} \right) \\ &+ \mathbf{e} \cdot \frac{2n}{\gamma \delta}. \end{aligned} \quad (68)$$

By choosing $\alpha \leq \rho_{\min}^{-1} (\frac{\delta_1}{2} (\theta + \eta) - \theta)^{-1}$ and (26), we observe that

$$\mathbf{c} \leq \rho_{\min}^{-1}. \quad (69)$$

To upper bound $\bar{\omega}_x$.

$$\begin{aligned} \bar{\omega}_x &\leq \frac{\alpha L^2}{n} - \mathbf{a} \cdot \frac{3}{2} \alpha \theta \rho_{\min} \\ &+ \mathbf{a} \cdot (8\alpha \eta \tilde{\rho}_{\max}^2 + 12\alpha^2 \eta^{-1} L^4) \rho_{\min}^{-1} + \mathbf{a} \cdot \frac{3\delta_1 \alpha}{2} \\ &+ \mathbf{a} \cdot \frac{4\delta_2}{\gamma \delta} [\alpha^2 \theta^2 (\rho_{\max}^2 + \sigma_A^2 \rho_{\max}/2) + \alpha^2 L^2]. \end{aligned} \quad (70)$$

It holds that $\omega_x \leq \frac{1}{4} \alpha \theta \rho_{\min} \mathbf{a} =: \omega_x < 0$, with

$$\begin{cases} \frac{\alpha L^2}{n} \leq \frac{1}{8} \alpha \theta \rho_{\min} \mathbf{a} & \Leftrightarrow \theta \geq \frac{8L^2}{\rho_{\min} n \mathbf{a}}, \\ 8\alpha \eta \tilde{\rho}_{\max}^2 \rho_{\min}^{-1} \leq \frac{1}{4} \alpha \theta \rho_{\min} & \Leftrightarrow \theta \geq 32\eta \tilde{\rho}_{\max}^2 \rho_{\min}^{-2}, \\ 12\alpha^2 \eta^{-1} L^4 \rho_{\min}^{-1} \leq \frac{1}{8} \alpha \theta \rho_{\min} & \Leftrightarrow \alpha \leq \frac{\theta \eta \rho_{\min}^2}{96L^4}, \\ \frac{3}{2} \delta_1 \alpha \leq \frac{3}{8} \alpha \theta \rho_{\min} & \Leftrightarrow \theta \geq 8\delta_1 \rho_{\min}^{-1}, \\ \frac{4\delta_2}{\gamma \delta} \alpha^2 \theta^2 \rho_{\max}^2 \leq \frac{1}{8} \alpha \theta \rho_{\min} & \Leftrightarrow \alpha \leq \frac{\gamma \delta \rho_{\min}}{32\delta_2 \theta \rho_{\max}^2}, \\ \frac{2\delta_2}{\gamma \delta} \alpha^2 \theta^2 \sigma_A^2 \rho_{\max} \leq \frac{1}{8} \alpha \theta \rho_{\min} & \Leftrightarrow \alpha \leq \frac{\gamma \delta \rho_{\min}}{16\delta_2 \theta \sigma_A^2 \rho_{\max}}, \\ \frac{4\delta_2}{\gamma \delta} \alpha^2 L^2 \leq \frac{1}{8} \alpha \theta \rho_{\min} & \Leftrightarrow \alpha \leq \frac{\gamma \delta \theta \rho_{\min}}{32\delta_2 L^2}. \end{cases} \quad (71)$$

To upper bound $\bar{\omega}_v$, using $\mathbf{c} \leq \rho_{\min}^{-1}$ leads to

$$\bar{\omega}_v \leq \mathbf{a} \cdot 3 + \mathbf{a} \cdot 4\rho_{\min}^{-1} \eta^{-1} + \mathbf{a} \cdot -\frac{1}{8} \delta_1 + \mathbf{a} \cdot \frac{4}{\gamma \delta} \delta_2. \quad (72)$$

It holds that $\omega_v \leq -\mathbf{a} \frac{1}{32} \delta_1 \leq -\mathbf{a} =: \omega_v < 0$, with

$$\begin{cases} 3 \leq \frac{1}{32} \delta_1 & \Leftrightarrow \delta_1 \geq 96, \\ 4\rho_{\min}^{-1} \eta^{-1} \leq \frac{1}{32} \delta_1 & \Leftrightarrow \delta_1 \geq 128\rho_{\min}^{-1} \eta^{-1}, \\ \frac{4}{\gamma \delta} \delta_2 \leq \frac{1}{32} \delta_1 & \Leftrightarrow \delta_1 \geq \frac{128}{\gamma \delta} \delta_2. \end{cases} \quad (73)$$

To upper bound $\bar{\omega}_{\hat{x}}$,

$$\begin{aligned} \bar{\omega}_{\hat{x}} &\leq \mathbf{a} \cdot 9\alpha \theta \tilde{\rho}_{\max}^2 \rho_{\min}^{-1} + \mathbf{a} \cdot 4\eta \tilde{\rho}_{\max}^2 \rho_{\min}^{-1} \\ &+ \mathbf{a} \cdot \frac{\delta_1}{2} (\alpha \eta^2 \rho_{\max}^2 + 5\alpha^2 \theta^2 \tilde{\rho}_{\max}^2) - \mathbf{a} \cdot \frac{\gamma \delta}{4} \delta_2. \end{aligned} \quad (74)$$

It holds that $\bar{\omega}_{\hat{x}} \leq -\frac{\gamma \delta}{16} \mathbf{a} =: \omega_{\hat{x}} < 0$, with

$$\begin{cases} 9\alpha \theta \tilde{\rho}_{\max}^2 \rho_{\min}^{-1} \leq \frac{\gamma \delta}{16} \delta_2 & \Leftrightarrow \alpha \leq \frac{\gamma \delta \delta_2 \rho_{\min}}{144\theta \tilde{\rho}_{\max}^2}, \\ 4\eta \tilde{\rho}_{\max}^2 \rho_{\min}^{-1} \leq \frac{\gamma \delta}{16} \delta_2 & \Leftrightarrow \delta_2 \geq \frac{64\eta \tilde{\rho}_{\max}^2}{\gamma \delta \rho_{\min}}, \\ \frac{\delta_1}{2} \alpha \eta^2 \rho_{\max}^2 \leq \frac{\gamma \delta}{32} \delta_2 & \Leftrightarrow \alpha \leq \frac{\gamma \delta \delta_2}{16\delta_1 \eta^2 \rho_{\max}^2}, \\ \frac{\delta_1}{2} 5\alpha^2 \theta^2 \tilde{\rho}_{\max}^2 \leq \frac{\gamma \delta}{32} \delta_2 & \Leftrightarrow \alpha \leq \frac{\sqrt{\gamma \delta \delta_2 / 80 \delta_1}}{\theta \tilde{\rho}_{\max}}. \end{cases} \quad (75)$$

To upper bound $\bar{\omega}_f$, notice that

$$\omega_f \leq -\frac{1}{4} \alpha + 12\mathbf{a} \alpha^2 \eta^{-1} \rho_{\min}^{-1} nL^2 + \frac{9}{2} \mathbf{a} \delta_1 \alpha^2 nL^2 + \mathbf{a} \frac{4\delta_2}{\gamma \delta} \alpha^2. \quad (76)$$

It holds that $\bar{\omega}_f \leq -\frac{1}{16} \alpha =: \omega_f < 0$, with

$$\begin{cases} 12\mathbf{a} \alpha^2 \eta^{-1} \rho_{\min}^{-1} nL^2 \leq \frac{1}{16} \alpha & \Leftrightarrow \alpha \leq \frac{\eta \rho_{\min}}{192nL^2 \mathbf{a}}, \\ \frac{9}{2} \mathbf{a} \delta_1 \alpha^2 nL^2 \leq \frac{1}{16} \alpha & \Leftrightarrow \alpha \leq \frac{1}{72\delta_1 nL^2 \mathbf{a}}, \\ \mathbf{a} \frac{4\delta_2}{\gamma \delta} \alpha^2 \leq \frac{1}{16} \alpha & \Leftrightarrow \alpha \leq \frac{\gamma \delta}{64\delta_2 \mathbf{a}}. \end{cases} \quad (77)$$

Lastly, the upper bound of $\bar{\omega}_\sigma$ is

$$\bar{\omega}_\sigma \leq \frac{L}{2n} + \mathbf{a} (n + 12 \frac{L^2}{\eta \rho_{\min}} + \frac{3\delta_1 \alpha}{2} (3L^2 + n) + \frac{2n\delta_2}{\gamma \delta}). \quad (78)$$

It holds that $\bar{\omega}_\sigma \leq \omega_\sigma$ under $\theta \geq \frac{8192\tilde{\rho}_{\max}}{\gamma \delta \rho_{\min}^2}$.

We notice that a sufficient condition to satisfying the above step size conditions is to set $\theta \geq \theta_{lb}$, $\alpha \leq \alpha_{ub}$ where

$$\begin{aligned} \theta_{lb} &= 4\rho_{\min}^{-1} \max\left\{ \frac{2L^2}{n\mathbf{a}}, \frac{2048\tilde{\rho}_{\max}}{\gamma \delta \rho_{\min}}, L^2 \right\}, \\ \alpha_{ub} &= \frac{\gamma \delta}{256\theta} \cdot \min\left\{ \frac{\rho_{\min}^2}{\rho_{\max}^2 \tilde{\rho}_{\max}}, \frac{\rho_{\min}^2}{\sigma_A^2 \rho_{\max} \tilde{\rho}_{\max}}, \right. \\ &\quad \left. \frac{1}{72n\mathbf{a}\tilde{\rho}_{\max}}, \frac{\rho_{\min}}{2\tilde{\rho}_{\max}\mathbf{a}} \right\}. \end{aligned} \quad (79)$$

This concludes the proof. \square

APPENDIX G AUXILIARY LEMMAS

Lemma G.1. *Under Assumption IV.1 and IV.2,*

$$\begin{aligned} &\mathbb{E} \left[\|\nabla \mathbf{f}(\mathbf{1}_{\otimes} \bar{\mathbf{x}}^{t+1}) - \nabla \mathbf{f}(\mathbf{1}_{\otimes} \bar{\mathbf{x}}^t)\|^2 \right] \\ &\leq 3\alpha^2 nL^2 \left\{ \frac{1}{n^2} \sum_{i=1}^n \sigma_i^2 + \mathbb{E} \left[\|\nabla \mathbf{f}(\bar{\mathbf{x}}^t)\|^2 \right] \right\} + 3\alpha^2 L^4 \|\mathbf{X}^t\|_{\mathbf{K}}^2. \end{aligned}$$

Proof. By the Lipschitz gradient assumption on each local objective function f_i ,

$$\begin{aligned} &\mathbb{E} \left[\|\nabla \mathbf{f}(\mathbf{1}_{\otimes} \bar{\mathbf{x}}^{t+1}) - \nabla \mathbf{f}(\mathbf{1}_{\otimes} \bar{\mathbf{x}}^t)\|^2 \right] \\ &\leq 3\alpha^2 nL^2 \mathbb{E} \left[\frac{1}{n^2} \sum_{i=1}^n \|\nabla f_i(\mathbf{X}_i^t; \xi_i^{t+1}) - \nabla f_i(\mathbf{X}_i^t)\|^2 \right] \\ &+ \mathbb{E} \left[\|\nabla \mathbf{f}(\bar{\mathbf{x}}^t)\|^2 + \frac{1}{n} \sum_{i=1}^n \|\nabla f_i(\mathbf{X}^t) - \nabla f_i(\bar{\mathbf{x}}^t)\|^2 \right] \\ &\leq 3\alpha^2 nL^2 \left\{ \frac{1}{n^2} \sum_{i=1}^n \sigma_i^2 + \mathbb{E} \left[\|\nabla \mathbf{f}(\bar{\mathbf{x}}^t)\|^2 \right] \right\} + 3\alpha^2 L^4 \|\mathbf{X}^t\|_{\mathbf{K}}^2. \end{aligned} \quad \square$$

REFERENCES

- [1] A. G. Dimakis, S. Kar, J. M. Moura, M. G. Rabbat, and A. Scaglione, "Gossip algorithms for distributed signal processing," *Proceedings of the IEEE*, vol. 98, no. 11, pp. 1847–1864, 2010.
- [2] L. Xiao, S. Boyd, and S.-J. Kim, "Distributed average consensus with least-mean-square deviation," *Journal of parallel and distributed computing*, vol. 67, no. 1, pp. 33–46, 2007.
- [3] S. Kar and J. M. Moura, "Consensus+ innovations distributed inference over networks: cooperation and sensing in networked systems," *IEEE Signal Processing Magazine*, vol. 30, no. 3, pp. 99–109, 2013.
- [4] G. Mateos, J. A. Bazerque, and G. B. Giannakis, "Distributed sparse linear regression," *IEEE Transactions on Signal Processing*, vol. 58, no. 10, pp. 5262–5276, 2010.
- [5] X. Lian, C. Zhang, H. Zhang, C.-J. Hsieh, W. Zhang, and J. Liu, "Can decentralized algorithms outperform centralized algorithms? a case study for decentralized parallel stochastic gradient descent," *Advances in neural information processing systems*, vol. 30, 2017.
- [6] A. Nedic and A. Ozdaglar, "Distributed subgradient methods for multi-agent optimization," *IEEE Transactions on Automatic Control*, vol. 54, no. 1, pp. 48–61, 2009.
- [7] W. Shi, Q. Ling, G. Wu, and W. Yin, "Extra: An exact first-order algorithm for decentralized consensus optimization," *SIAM Journal on Optimization*, vol. 25, no. 2, pp. 944–966, 2015.
- [8] G. Qu and N. Li, "Harnessing smoothness to accelerate distributed optimization," *IEEE Transactions on Control of Network Systems*, vol. 5, no. 3, pp. 1245–1260, 2017.
- [9] J. Zeng and W. Yin, "On nonconvex decentralized gradient descent," *IEEE Transactions on signal processing*, vol. 66, no. 11, pp. 2834–2848, 2018.
- [10] D. Hajinezhad and M. Hong, "Perturbed proximal primal–dual algorithm for nonconvex nonsmooth optimization," *Mathematical Programming*, vol. 176, no. 1, pp. 207–245, 2019.
- [11] X. Yi, S. Zhang, T. Yang, T. Chai, and K. H. Johansson, "Linear convergence of first-and zeroth-order primal–dual algorithms for distributed nonconvex optimization," *IEEE Transactions on Automatic Control*, vol. 67, no. 8, pp. 4194–4201, 2021.
- [12] T.-H. Chang, M. Hong, H.-T. Wai, X. Zhang, and S. Lu, "Distributed learning in the nonconvex world: From batch data to streaming and beyond," *IEEE Signal Processing Magazine*, vol. 37, no. 3, pp. 26–38, 2020.
- [13] A. Nedić and A. Olshevsky, "Distributed optimization over time-varying directed graphs," *IEEE Transactions on Automatic Control*, vol. 60, no. 3, pp. 601–615, 2014.
- [14] A. Nedic, A. Olshevsky, and W. Shi, "Achieving geometric convergence for distributed optimization over time-varying graphs," *SIAM Journal on Optimization*, vol. 27, no. 4, pp. 2597–2633, 2017.
- [15] W. Wen, C. Xu, F. Yan, C. Wu, Y. Wang, Y. Chen, and H. Li, "Terngrad: Ternary gradients to reduce communication in distributed deep learning," *Advances in neural information processing systems*, vol. 30, 2017.
- [16] C. M. De Sa, C. Zhang, K. Olukotun, and C. Ré, "Taming the wild: A unified analysis of hogwild-style algorithms," *Advances in neural information processing systems*, vol. 28, 2015.
- [17] J. Dean, G. Corrado, R. Monga, K. Chen, M. Devin, M. Mao, M. Ranzato, A. Senior, P. Tucker, K. Yang, *et al.*, "Large scale distributed deep networks," *Advances in neural information processing systems*, vol. 25, 2012.
- [18] F. Seide, H. Fu, J. Droppo, G. Li, and D. Yu, "1-bit stochastic gradient descent and its application to data-parallel distributed training of speech dnns," in *Interspeech*, vol. 2014, pp. 1058–1062, Singapore, 2014.
- [19] P. Richtárik, I. Sokolov, and I. Fatkhullin, "Ef21: A new, simpler, theoretically better, and practically faster error feedback," *Advances in Neural Information Processing Systems*, vol. 34, pp. 4384–4396, 2021.
- [20] A. Reiszadeh, A. Mokhtari, H. Hassani, and R. Pedarsani, "An exact quantized decentralized gradient descent algorithm," *IEEE Transactions on Signal Processing*, vol. 67, no. 19, pp. 4934–4947, 2019.
- [21] S. Magnússon, H. Shokri-Ghadikolaei, and N. Li, "On maintaining linear convergence of distributed learning and optimization under limited communication," *IEEE Transactions on Signal Processing*, vol. 68, pp. 6101–6116, 2020.
- [22] X. Liu and Y. Li, "Linear convergent decentralized optimization with compression," in *International Conference on Learning Representations*, 2021.
- [23] H. Zhao, B. Li, Z. Li, P. Richtárik, and Y. Chi, "Beer: Fast $o(1/t)$ rate for decentralized nonconvex optimization with communication compression," *Advances in Neural Information Processing Systems*, vol. 35, pp. 31653–31667, 2022.
- [24] A. Koloskova, S. Stich, and M. Jaggi, "Decentralized stochastic optimization and gossip algorithms with compressed communication," in *International Conference on Machine Learning*, pp. 3478–3487, PMLR, 2019.
- [25] A. Koloskova, T. Lin, S. U. Stich, and M. Jaggi, "Decentralized deep learning with arbitrary communication compression," in *Proceedings of the 8th International Conference on Learning Representations*, 2019.
- [26] C.-Y. Yau and H.-T. Wai, "Docom: Compressed decentralized optimization with near-optimal sample complexity," *arXiv preprint arXiv:2202.00255*, 2022.
- [27] A. Xie, X. Yi, X. Wang, M. Cao, and X. Ren, "A communication-efficient stochastic gradient descent algorithm for distributed nonconvex optimization," *arXiv preprint arXiv:2403.01322*, 2024.
- [28] C.-Y. Yau, H. Liu, and H.-T. Wai, "Fully stochastic primal-dual gradient algorithm for non-convex optimization on random graphs," *arXiv preprint arXiv:2410.18774*, 2024.
- [29] K. Srivastava and A. Nedic, "Distributed asynchronous constrained stochastic optimization," *IEEE journal of selected topics in signal processing*, vol. 5, no. 4, pp. 772–790, 2011.
- [30] H. Reiszadeh, B. Touri, and S. Mohajer, "Dimix: Diminishing mixing for sloppy agents," *SIAM Journal on Optimization*, vol. 33, no. 2, pp. 978–1005, 2023.
- [31] R. Nassif, S. Vlaski, M. Carpentiero, V. Matta, and A. H. Sayed, "Differential error feedback for communication-efficient decentralized optimization," in *2024 IEEE 13rd Sensor Array and Multichannel Signal Processing Workshop (SAM)*, pp. 1–5, IEEE, 2024.
- [32] N. Michelusi, G. Scutari, and C.-S. Lee, "Finite-bit quantization for distributed algorithms with linear convergence," *IEEE Transactions on Information Theory*, vol. 68, no. 11, pp. 7254–7280, 2022.
- [33] R. Nassif, S. Vlaski, M. Carpentiero, V. Matta, M. Antonini, and A. H. Sayed, "Quantization for decentralized learning under subspace constraints," *IEEE Transactions on Signal Processing*, vol. 71, pp. 2320–2335, 2023.
- [34] A. S. Mathkar and V. S. Borkar, "Nonlinear gossip," *SIAM Journal on Control and Optimization*, vol. 54, no. 3, pp. 1535–1557, 2016.
- [35] H. Liu, C.-Y. Yau, and H.-T. Wai, "A two-timescale primal-dual algorithm for decentralized optimization with compression," in *ICASSP*, 2025.
- [36] C.-Y. Yau and H.-T. Wai, "Fully stochastic distributed convex optimization on time-varying graph with compression," in *2023 62nd IEEE Conference on Decision and Control (CDC)*, pp. 145–150, IEEE, 2023.
- [37] D. Alistarh, D. Grubic, J. Li, R. Tomioka, and M. Vojnovic, "Qsgd: Communication-efficient sgd via gradient quantization and encoding," *Advances in neural information processing systems*, vol. 30, 2017.